NAVAL POSTGRADUATE SCHOOL

MONTEREY, CALIFORNIA

THESIS

DEVELOPMENT AND TESTING OF A HYBRID WHEG™-MOBILE PLATFORM FOR AUTONOMOUS SURF-ZONE OPERATIONS

by

Michael Slatt

December 2011

Thesis Advisor: Richard Harkins
Second Reader: Peter Crooker

Approved for public release; distribution is unlimited

THIS PAGE INTENTIONALLY LEFT BLANK

REPORT DOCUMENTATION PAGE

Form Approved
OMB No. 0704–0188

1. REPORT DATE *(DD–MM–YYYY)*	2. REPORT TYPE	3. DATES COVERED *(From — To)*
8–12–2011	Master's Thesis	9/28/2009–12/16/2011

4. TITLE AND SUBTITLE

Development and Testing of a Hybrid Wheg™-Mobile Platform for Autonomous Surf-Zone Operations

5a. CONTRACT NUMBER

5b. GRANT NUMBER

5c. PROGRAM ELEMENT NUMBER

6. AUTHOR(S)

Michael Slatt

5d. PROJECT NUMBER

5e. TASK NUMBER

5f. WORK UNIT NUMBER

7. PERFORMING ORGANIZATION NAME(S) AND ADDRESS(ES)

Naval Postgraduate School
Monterey, CA 93943

8. PERFORMING ORGANIZATION REPORT NUMBER

9. SPONSORING / MONITORING AGENCY NAME(S) AND ADDRESS(ES)

Department of the Navy

10. SPONSOR/MONITOR'S ACRONYM(S)

11. SPONSOR/MONITOR'S REPORT NUMBER(S)

12. DISTRIBUTION / AVAILABILITY STATEMENT

Approved for public release; distribution is unlimited

13. SUPPLEMENTARY NOTES

The views expressed in this thesis are those of the author and do not reflect the official policy or position of the Department of Defense or the U.S. Government. **IRB Protocol Number: XXXX**

14. ABSTRACT

Mobility Over Non-Trivial Terrain (MONTe) is a hybrid (wheel-leg) Wheg™-mobile platform created for two purposes. The first purpose is to verify the simulated benefits of adapting previous six-legged Wheg robotic platforms to a four-legged Wheg amphibious design with a tail. The second purpose is to provide a platform to continue autonomous design and testing in the amphibious environment. In addition, the challenges of previous NPS surf-zone designs are investigated as well as the new challenges of making an amphibious platform to include the following: suspension system, drivetrain, tail integration, environmental control for subsystems, power distribution system and water-borne operation.

15. SUBJECT TERMS

16. SECURITY CLASSIFICATION OF:			17. LIMITATION OF ABSTRACT	18. NUMBER OF PAGES	19a. NAME OF RESPONSIBLE PERSON
a. REPORT	b. ABSTRACT	c. THIS PAGE			19b. TELEPHONE NUMBER *(include area code)*
Unclassified	Unclassified	Unclassified	UU	75	

THIS PAGE INTENTIONALLY LEFT BLANK

Approved for public release; distribution is unlimited

DEVELOPMENT AND TESTING OF A HYBRID WHEG™-MOBILE PLATFORM FOR AUTONOMOUS SURF-ZONE OPERATIONS

Michael Slatt
Major, United States Marine Corps
B.S., U.S. Naval Academy, 2000

Submitted in partial fulfillment of the
requirements for the degree of

MASTER OF SCIENCE IN APPLIED PHYSICS

from the

NAVAL POSTGRADUATE SCHOOL
December 2011

Author: Michael Slatt

Approved by: Richard Harkins
Thesis Advisor

Peter Crooker
Second Reader

Andres Larraza
Chair, Department of Physics

THIS PAGE INTENTIONALLY LEFT BLANK

ABSTRACT

Mobility Over Non-Trivial Terrain (MONTe) is a hybrid (wheel-leg) Wheg™-mobile platform created for two purposes. The first purpose is to verify the simulated benefits of adapting previous six-legged Wheg robotic platforms to a four-legged Wheg amphibious design with a tail. The second purpose is to provide a platform to continue autonomous design and testing in the amphibious environment. In addition, the challenges of previous NPS surf-zone designs are investigated as well as the new challenges of making an amphibious platform to include the following: suspension system, drivetrain, tail integration, environmental control for subsystems, power distribution system and water-borne operation.

THIS PAGE INTENTIONALLY LEFT BLANK

Contents

Appendices

List of Figures

Acknowledgements

I would like to thank: my wife Pamela for allowing me to escape to Never Never Land and not holding it against me when I returned, my advisor Richard Harkins for the freedom he gave me to run with his project, my second reader Peter Crooker for his attention to detail and willingness to go the extra mile, my former group members Jason Hickle and Steve Halle for their parts in creating MONTe, George Jaksha for his mentorship in the machine shop and friendship outside it, Dan Sakoda for his constant help with 3D printing, Sam Barone for help with lab equipment and electronics expertise, my brother Ed and his company PCBsingles.com, Matt Ryan from Ryan Mechatronis, and Matt Klein and Alex Boxerbaum of Case Western University for their insightful discussions along the way.

THIS PAGE INTENTIONALLY LEFT BLANK

CHAPTER 1:
Introduction

The NPS Small Robotic Technology (SMART) initiative was started in the Physics Department of the Naval Postgraduate School in 2001 [1]. The SMART initiative identified a requirement to study robotics for use and integration into existing and future DoD missions.

Robots have become ordinary in many sectors of life. Some robots are able to wash our clothes while others can disable improvised explosive devices (IEDs). Robots complete specific tasks which are often trivial, time consuming, or dangerous, and do so extremely efficiently and reliably. The challenge in robotics is to build systems that are capable of multiple tasks while doing so competently. A robot capable of operating in the surf-zone environment is one such example of a multi-tasked robot.

Littoral zones are important today in the framework of national security and will continue to be important in the future as the world's population gravitates to coastal regions [2]. Advancing our use of robotics in this environment will ensure we are ready to meet future challenges such as piracy, mine detection and surveillance of commerce choke points. The development and testing of our robot, named Mobility Over Non-trivial Terrain (MONTe), is one more step in this direction.

1.1 NPS Surf-Zone Robot History

1.1.1 Track-Mobile Platform

In 2001, the NPS Surf-Zone Robotic program began with Bender, Figure 1.1. The robot was built on a Foster Miller Lemming tracked platform acquired from the Coastal Systems Station (CSS) Naval research facility in Panama City, Florida.

The Foster Miller platform was modified by adding a compartment to the top of the chassis for a microprocessor and sensors. The platform had independently actuated left and right tracks so that directional control was accomplished through differential track speeds. The classic tank drive allowed the platform to perform zero-radius turns. This version of the surf-zone robot was not watertight. Consequently, experiments in the surf-zone were limited. Up until 2005, succeeding theses improved Bender's systems and controls and invoked autonomy for land-borne operatons.

Figure 1.1: From [3], Bender.

1.1.2 Wheg-Mobile Platform

In 2005, the SMART initiative group teamed up with Case Western Reserve University and the concept of Wheg-mobility was first introduced to NPS [3]. Case Western's team of master's and doctorate students under the lead of Roger Quinn were at that time, and are still today, leading innovators in the subject of biologically inspired robots. Case Western created the Wheg which allowed them to mimic certain mobility modes discovered in the study of cockroaches [4]. While studying the mobility of a cockroach, specifically its ability to climb obstacles, the importance of a body joint capable of changing the location of its center of mass was discovered and implemented into the design of many of the Wheg-mobile platforms. An example is shown in Figure 1.2.

Figure 1.2: From [6], an example of a body joint.

Prior to 2009, the Wheg-mobile robots designed by Case Western had several similarities. Most had the following characteristics and can be observed in Figure 1.3 [5]:

- six-legged
- three-spoked Whegs
- mechanical Wheg compliance component for phase changing
- Ackermann steering geometry in the front and rear sets of Whegs
- single-motor driven
- RC type manual control of actuators using pulse-width modulation (PWM)

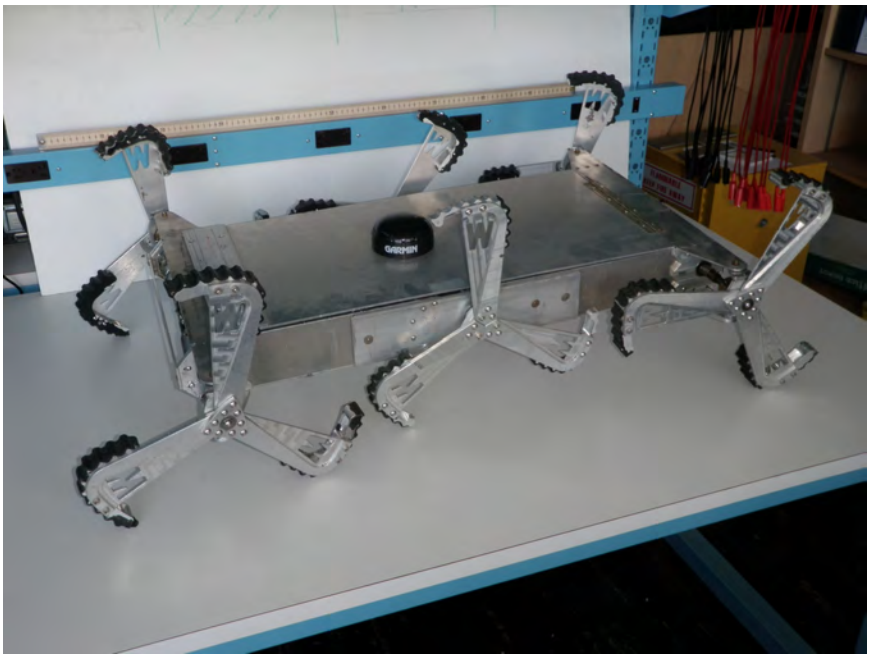

Figure 1.3: From [5], Agbot.

1.1.3 Hybrid Wheg-Mobile Platform

In 2009, a hybrid concept of mobility was introduced in a joint paper by NPS and Case Western [6]. The platform continued the use of Whegs, but replaced the rear set of Whegs with a tail. Ackerman steering was also dropped and replaced with differential steering similar to the tracked-mobile platform discussed previously. Hybrid Wheg-mobile platforms are synonymous with the rendering of the concept named Pelican Whegs, Figure 1.4.

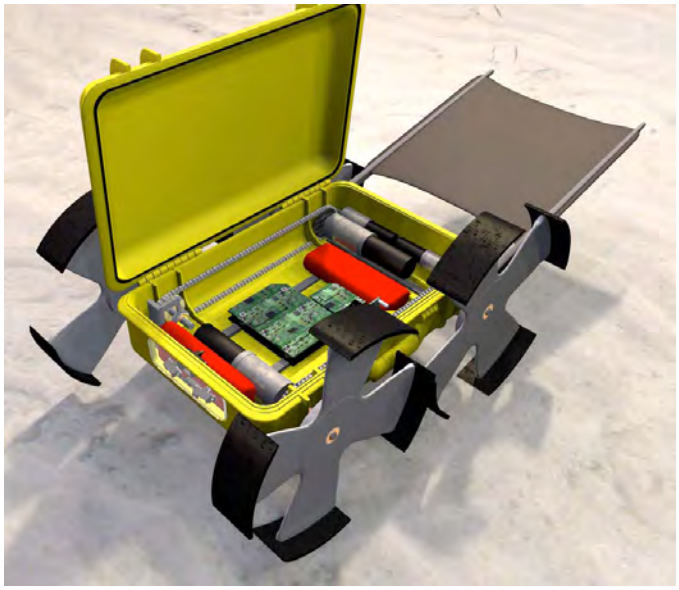

Figure 1.4: From [6], the rendering of a hybrid Wheg-mobile platform called Pelican Whegs.

Simulations conducted by Case Western showed that by adding a tail in place of the rear set of Whegs, the robot was able to traverse higher obstacles than the previous six-legged designs. Simulations demonstrated that the robot with four Whegs and a tail was able to climb an obstacle six centimeters higher than a similar robot with six Whegs [6].The addition of a tail shifted the center of mass forward with respect to the body joint, Figure 1.2 and 1.5. This helped the platform gain traction once on top of the obstacle and prevented the platform from losing ground by slipping backward.

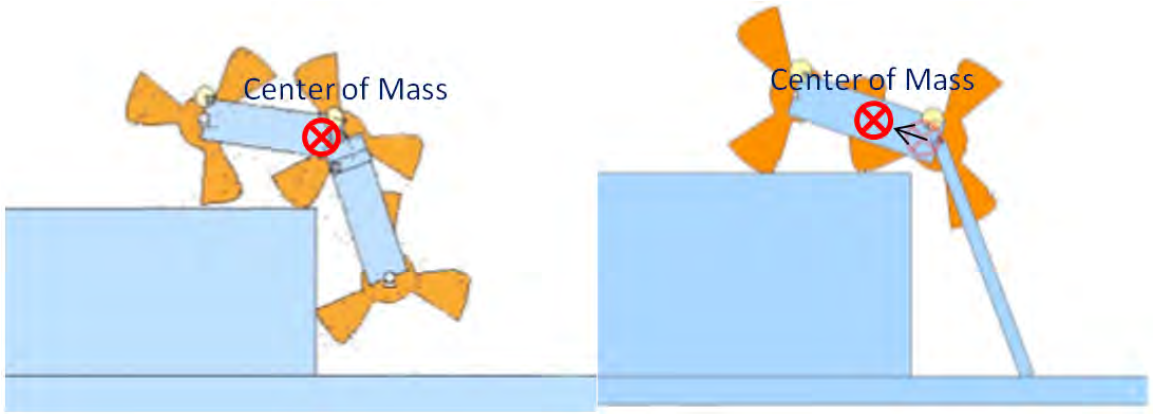

Figure 1.5: From [6], 2D simulations comparing a six-legged robot to a 4-legged robot with a tail.

NPS Hybrid Wheg-Mobile Platform Version 1 - ROBSTER

In 2009, NPS created their first version of a hybrid Wheg-mobile platform named ROBSTER, Figure 1.6 [7]. ROBSTER was a platform specifically built to allowl tail control.

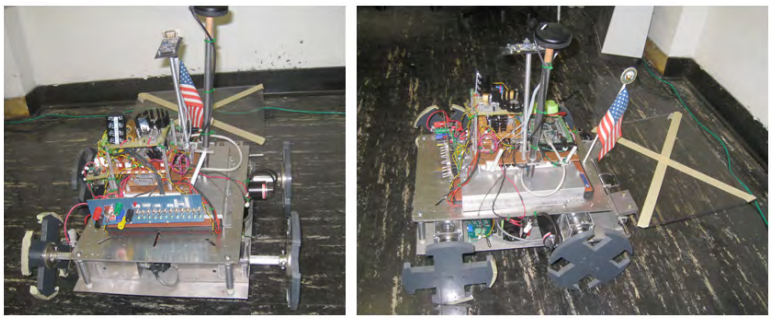

Figure 1.6: From [7], ROBSTER viewed from the front and left side.

NPS Hybrid Wheg-Mobile Platform Version 2 - MONTe

In 2010, NPS began creating their second version ofthe Hybrid Wheg-mobile platform, named Mobility Over Non-trivial Terrain (MONTe), Figure 1.7. MONTe builds on the lessons learned from ROBSTER but does so as an entirely new platform. The platform and internals have all been upgraded to include processors, sensors, the power distribution system, and the operating system which ties it all together. An in depth discussion of the implementation of a Robotic Operating System (ROS), communications scheme, initial tail modeling, and sensor handling for MONTe can be found in [8].

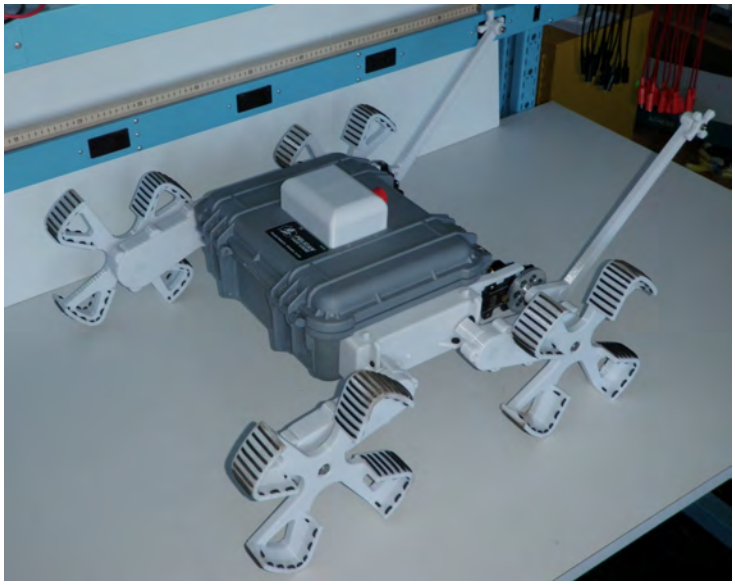

Figure 1.7: MONTe.

1.2 Concept of Operation

The typical mission for MONTe could be the following:

1. MONTe would be deployed subsurface as a single platform or as part of a swarm.
2. MONTe would float to the surface and "swim" to the beach utilizing Seaweb as a source for navigation [9].
3. Once beached, MONTe would autonomously navigate to a preplanned set of interest points and collect data from the sensor-package on board.
4. Data collected would be communicated wirelessly to an airborne UAV for retransmission to controlling and monitoring assets.
5. MONTe would allow for updates to the current mission or manual control as required.
6. On station time would be approximately 1.5 hours. Once MONTe's mission was complete or shortly before depleting all its energy, MONTe would return to the water to expire.

1.3 Related Work

Generally speaking, there are three main schemes currently being implemented for amphibious platforms. The separation between these schemes can be broken down to how the platforms accomplish water-mobility: floaters, bottom walkers and neutrally buoyant swimmers.

Tier One - Floaters and Bottom Walkers

Tier One amphibious platforms are either positively or negatively buoyant. MONTe was designed to be a positively buoyant platform in order to simplify current navigation schemes. Case Western's concurrent work on a hybrid Wheg-mobile platform was designed to be negatively buoyant in order to walk along the seabed, Figure 1.8.

Tier Two - Neutrally Buoyant Swimmers

Tier Two amphibious platforms are able to change depth and operate throughout the envelope defined by the top and bottom of a body of water. They are able to capitalize on favorable postures for energy conservation, concealment, communication, etc. Figure 1.9 shows two examples of Tier Two amphibious platforms [10],[11].

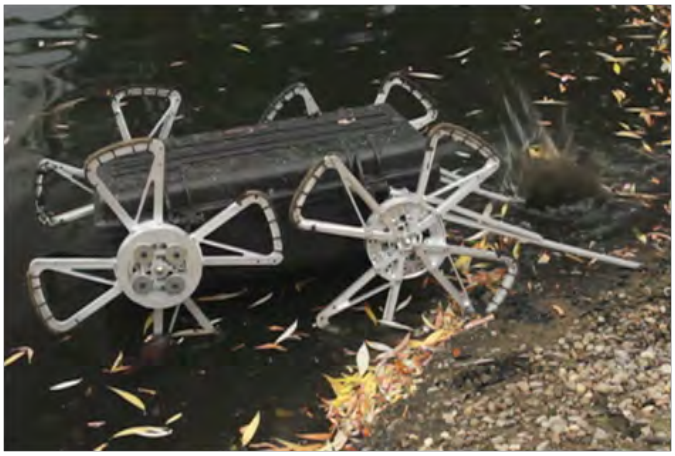

Figure 1.8: SeaDog, a creation of Matt Klein's from Case Western.

Figure 1.9: Left to right, McGill and York University's Aqua [10] and Boston Dynamics'Rhex [11].

THIS PAGE INTENTIONALLY LEFT BLANK

CHAPTER 2:
Concepts

2.1 Mobility and Suspension

The mobility of MONTe in difficult terrain is realized by the unique design of the Wheg. It provides the power efficiency of wheel performance in relatively flat terrain, but also enables the platform to climb as a human would climb steps, see Figures 2.1, 2.2 and 2.3.

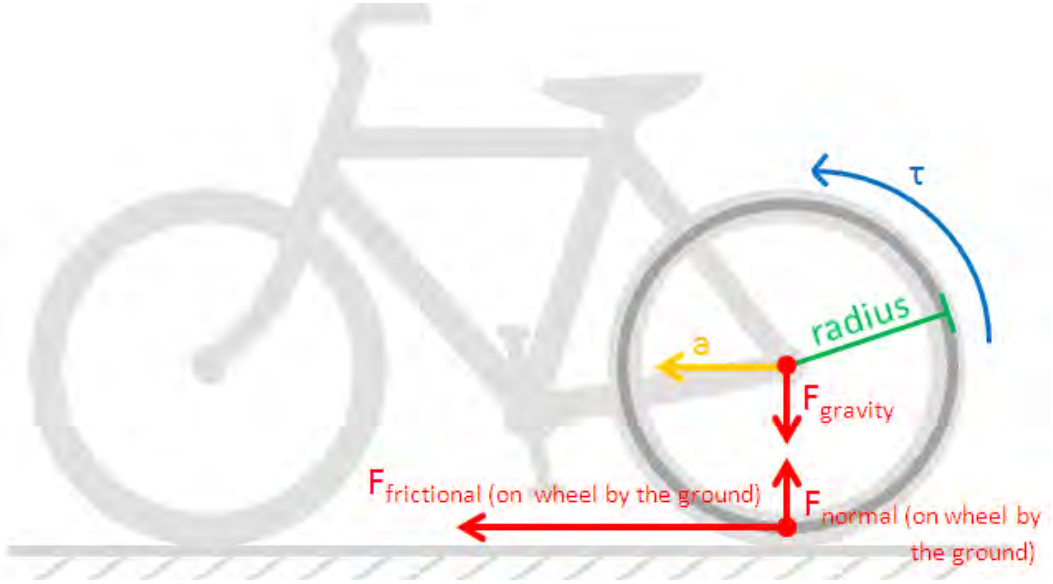

Figure 2.1: Force body diagram of a wheel.

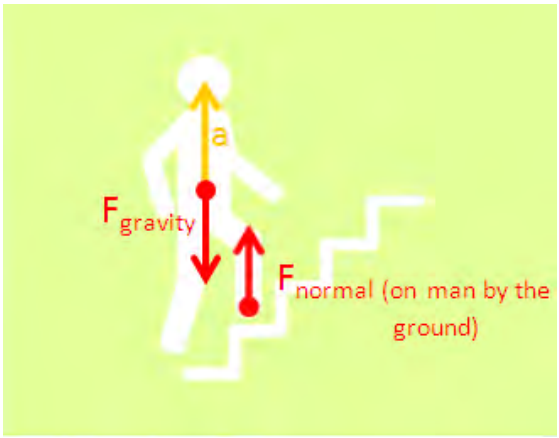

Figure 2.2: Force body diagram of a person climbing stairs.

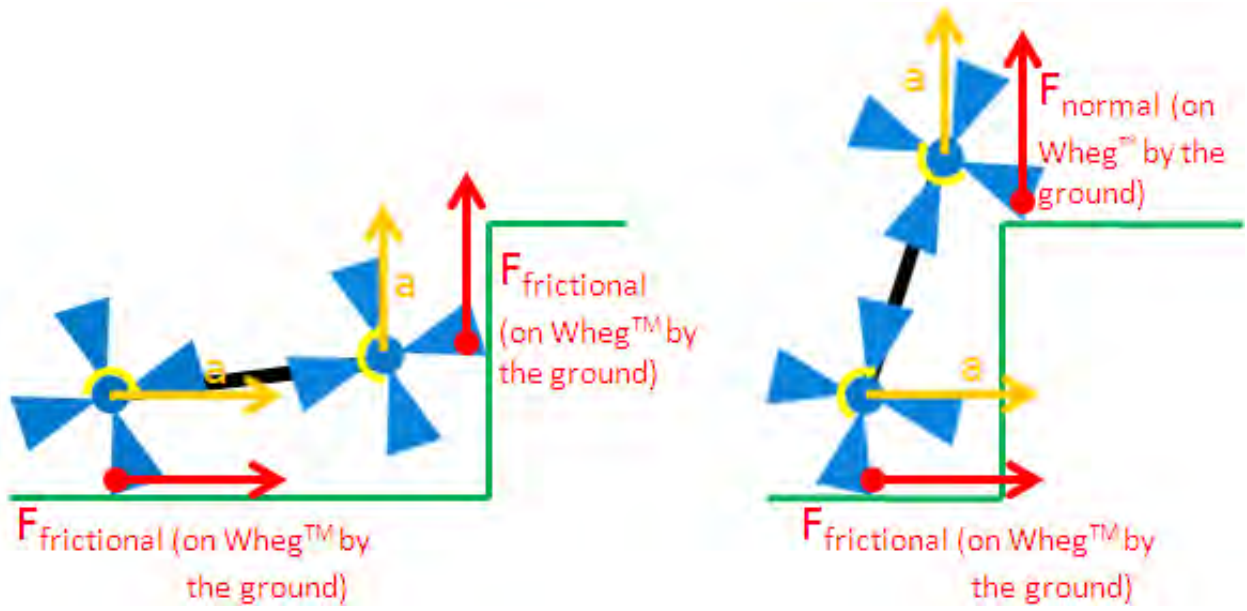

Figure 2.3: Left, Whegs beginning to traverse an obstacle like a normal wheel. Right: Whegs climbing like a wheel and like a person climbing stairs.

The downside to the Wheg is that the shape of the Wheg imparts a periodic forcing function to the platform as depicted in Figure 2.4.

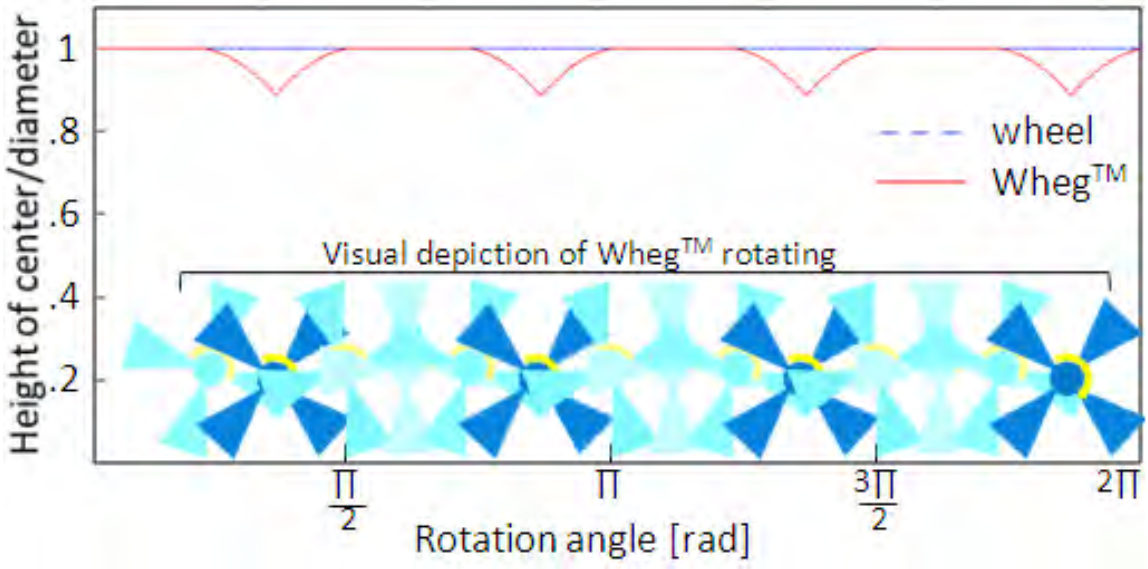

Figure 2.4: Plot of the height of center above ground vs. rotation angle for a wheel and Wheg.

This undamped periodic force has a tendency to pop rivets, back out screws, and wiggle loose electrical connections over extended periods of use. To minimize this effect, a suspension system is required. The mechanical suspension for MONTe can be modeled as a damped driven

mechanical system, see Figure 2.5 [12]. Here, a mass m is supported by a spring with spring constant k and damping coefficient b. If the mass is subjected to driving force $F(t)$, its vertical position z is given by:

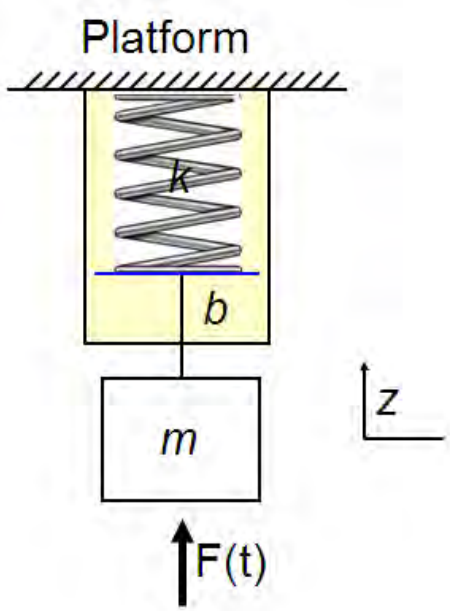

Figure 2.5: Damped driven harmonic motion diagram.

$$\ddot{z} + 2\beta\dot{z} + \omega_0^2 z = f(t), \tag{2.1}$$

where

$$2\beta = \frac{b}{m}, \tag{2.2}$$

$$\omega_0 = \sqrt{\frac{k}{m}}, \tag{2.3}$$

and

$$f(t) = \frac{F(t)}{m}. \tag{2.4}$$

Equation 2.2 defines the damping constant β, Equation 2.3 gives the natural angular frequency ω_0, and Equation 2.4 defines the normalized driving force $f(t)$. Equation 2.1 is a 2nd order differential equation that defines the equation of motion for the system.

The particular solution Equation 2.5 is:

$$x_{particular}(t) = A\cos(\omega t - \delta), \tag{2.5}$$

where

$$A = \frac{f_0}{\sqrt{(\omega_0^2 - \omega^2)^2 + 4\beta^2\omega^2}}, \tag{2.6}$$

and

$$\delta = \arctan\frac{2\beta\omega}{\omega_0^2 - \omega^2}, \tag{2.7}$$

where ω is the driving angular frequency in rad/s. If we plot the squared amplitude A^2 as a function of angular frequency, Figure 2.6:

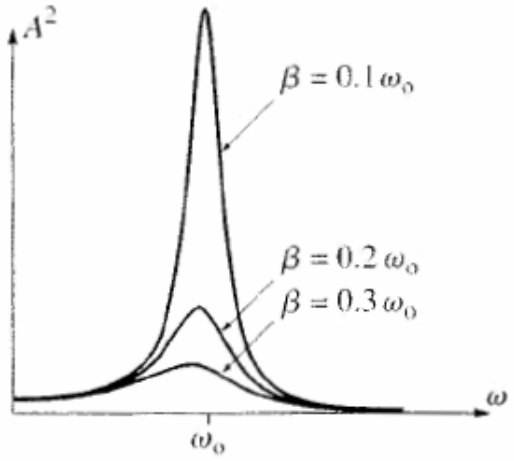

Figure 2.6: From [12], a plot of the squared amplitude as a function of driving freqency.

we notice that we can force the amplitude to zero by either driving off resonance or by increasing

the damping coefficient β. In order to produce a critically damped homogenous solution, we choose β to equal ω_0 and reduce the effects it has on the amplitude by driving the system off resonance.

The results of this analysis will be discussed in Chapter 4.

2.2 The Drivetrain

To provided enough torque for mobility, we have to overcome the internal and external equivalent inertia, J_{eq}, and friction, F_{eq}, as illustrated in Equations 2.8 and 2.9.

J_a and F_a are armature inertia and friction while J_l and F_l are load inertia and friction. We notice that we can minimize load friction and inertia by the proper selection of the gear ratio N.

$$J_{eq} = J_a + \frac{1}{N^2} J_l \tag{2.8}$$

$$F_{eq} = F_a + \frac{1}{N^2} F_l \tag{2.9}$$

2.3 Quasi-Closed System

The surf-zone environment can be extremely unforgiving to electronics and materials. Keeping sand and saltwater out of the robot is one requirement for operating in such an environment, but doing so can create a quasi-closed system. A quasi-closed system in the context of this thesis is defined to be a system that cannot easily transfer energy or matter across boundaries. Preventing matter from crossing boundaries is desired, however preventing energy from crossing boundaries is not. Electrical components such as processors, actuators, power supplies, batteries all create energy in the form of heat. Physical boundaries designed to keep water and sand out will result in a rise in temperature if they do not radiate heat at the same rate the components within those boundaries generate heat. This process is governed by the basic heat balance equation.

$$W = G\Delta T + C\frac{d}{dt}\Delta T \tag{2.10}$$

where G is the thermal conductance in W/°C, ΔT is the system change in temperature in °C, and C is the thermal capacitance in Ws/°C. Equation 2.10 relates the effects that adding power into

a system has on the temperature of the system. The maximum change in temperature ΔT_{max} occurs when the system reaches a steady-state condition as follows:

$$\Delta T_{max} = \frac{W}{G} \tag{2.11}$$

The power provided by the batteries to all the electrical components that is not converted to power in the drivetrain, $P_{drivetrain} = \tau\omega$, will vary the temperature within the quasi-closed system. The maximum change in temperature defined in Equation 2.11 can be reduced either by making the electronics and actuators more efficient, reducing the power W, or by increasing the net thermal conductance G of the boundary.

2.4 Noise Suppression

Electronic noise is something one can never get away from if using electronics. Whether Johnson, shot noise, generation-recombination or $\frac{1}{f}$, the goal is to decrease the noise or prohibit it from interfering with the intended circuit function. Characteristics of a robust power distribution scheme will be discussed without discussing the finer details of electronic noise.

Electric motors and actuators in general are usually very noisy electronic devices. In addition, the power driving circuits or schemes to power actuators can create noise as well. Microprocessors and sensors tend not to work well with noise. Information from sensors can be very easily lost if the noise from an actuator is allowed to bleed into the sensing circuit. Some processors will not function at all if they do not receive clean, uninterrupted power.

2.4.1 Power/Control Buss Isolation

One of the many steps in creating a robust power distribution system is to isolate the power (actuator) circuits from all other circuits electronically while maintaining the exchange of information. Information can be passed between the isolated busses in other ways then by current in wires. The use of light is one such way, which is how an optoisolator works, Figure 2.7 [13]. In addition to the means of communication, the format of the data can also help the exchange of information, i.e., digital vs. analog.

2.4.2 Noise Suppression Design Considerations

The close proximity of various hardware components in robotic systems can also create noise problems. The noise from a motor can bleed into other circuits even if the circuits are elec-

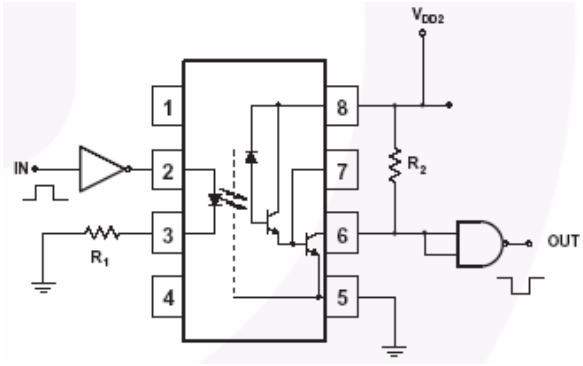

Figure 2.7: From [13], an optoisolator schematic.

tronically isolated by means of induction. Some steps can be taken to prevent magnetic fields from inducing currents in other circuit. Magnetic fields can be decreased or stopped through design and materials. A quick study of the toroid, used for filtering, will reveal a reduction of the magnetic field created on account of its geometry. The use of a conducting material to form a Faraday cage around motors is an example of using material characteristics to isolate magnetic fields. One can also attenuate magnetic fields simply by twisting wires carrying significant currents.

THIS PAGE INTENTIONALLY LEFT BLANK

CHAPTER 3:
Design

3.1 The Framework for Design

The development of MONTe addressed previous design problems and anticipated future challenges. Priorities of the design were as follows in the order of importance:

- Functionality
- Modularity
- Ruggedness

The characteristic of being functional is the most important because many of the problems one faces in building a robot is making all the systems work together. If the robot does not function similar to the intended design, it is hard to check the interoperability between systems or controlling schemes. The design of MONTe is modular because the robot was built in stages. Being modular gives the design flexibility to incorporate changes when initial assumptions are incorrect. Ruggedness deals with the ability of the platform to operate without constantly requiring maintenance. A robot that is rugged works longer and makes it easier to test.

3.1.1 Identified Problems of Previous Platforms

Wheg-Vibrations

Wheg geometry introduced periodic vibrations to the platform body. These undamped vibrations loosened screws, backed out rivets and caused electrical connections to fail. A suspension system was required to address these issues.

Electronics and Inter-Electronics Communication

Other problems with previous designs included issues with electronics communication devices:

- Processors: Image detection was accomplished on previous platforms, however, the lack of processing power prohibited the processing code from being completed onboard. In addition to the requirement for off-board processing, the communications protocol did not allow for the code to be run and returned to the platform in a real-time fashion [14].

- Electronics: The electronics previously used lacked the functionality, efficiency and compactness of modern electronics. One example would be the voltage regulators used on previous designs. Unlike modern switching power supplies, they are extremely inefficient and would heat up the quasi-closed system above maximum operating temperatures within minutes.

- Inter-electronics communications: The communication between electronic devices was inefficient and relied on external circuitry. One such example of this would be using the DAC output of a microprocessor to vary the duty cycle of square wave used as a PWM input to a RC motor controller. Although effective, the requirement for calibration as well as external circuitry had its shortcomings.

Future designs would incorporate more powerful processors and electronics with more flexibility and functionality.

3.1.2 Challenges Identified for the Current Design

Waterproofing

Previous NPS robot platforms, with the exception of Bender, were not designed to be waterproof. Waterproofing these designs after the fact would have been extremely challenging. Most of the design of MONTe was based upon the ability to waterproof the final design.

Platform Mechanical Development

The mechanics of the drivetrain and suspension were designed to be waterproof. Most of the mechanical components were fabricated as prototypes using in-house capabilities. The main challenge of the platform mechanical development was the ability to create a platform capable of proof-of-concept without an in-depth mechanical and material analysis.

Tail Integration

Adding a tail to previous designs was another challenge identified in the design of MONTe. Size, location, function, method of driving, and control were just a few of the variables in tail implementation.

Onboard Diagnostics

Based on the requirement to make the platform watertight; the ability to monitor and control internal diagnostics, specifically internal temperature, was important. An upgrade in process-

ing power was accompanied by an increase in heat generation. This required some means of efficient energy exchange to prevent damage to processor and other electronic components.

3.1.3 Land vs. Water

MONTe was designed as a platform, primarily land-based, with limited amphibious capabilities. The affects of this decision will be discussed throughout this chapter and the next.

3.2 The Design of MONTe

MONTe was designed using the 3D CAD design software program IronCAD. Figure 3.1 is an IronCAD 3D rendering of MONTe.

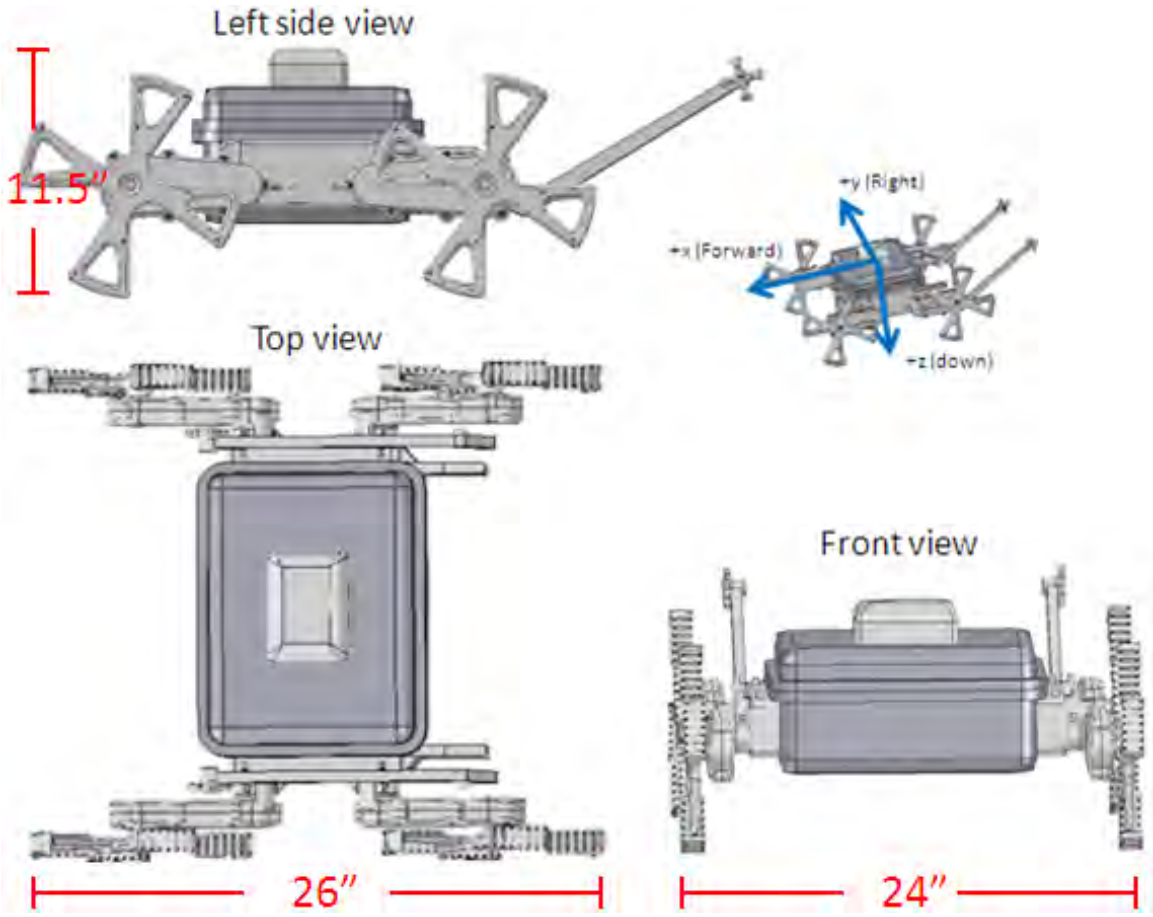

Figure 3.1: Isometric view of MONTe.

3.2.1 Mechanical

Materials and Fabrication

The fasteners, driveshafts, bearings and springs used in MONTe are all stainless. The exposed area of the platform is either polypropylene copolymer (Pelican case), polycarbonate (external modules) or aluminum (bottom heat sink). The seals which seal the modules to the case are made out of EPDM rubber.

Common fabrication techniques were used to build the platform, including lathe work and both manual and CNC milling. MONTe also capitalizes on resident NPS 3D printing knowledge and equipment (Fortus 400ms). The use of 3D printing equipment facilitated rapid prototyping. However, it must be stated that polycarbonate is not the preferred material for some of the parts because it does not stand up to impact forces as well as metals. Polycarbonate is brittle and breaks if stressed beyond its yield point.

Chassis

MONTe was built around a COTS Pelican 1400 watertight case, Figure 3.2. It was selected based on the reliability of the main enclosure seal. Previous testing, completed by Case Western, highlighted deficiencies in the Pelican case's ability to seal at modest depths. However, the case was chosen because the robot would only be underwater for a short duration.

The case measures roughly 13.5x11.5x6.0 inches and displaces enough water to support approximately 20 lbs. Based on the symmetry of the case and the goal of implementing a suspension system, the design was planned with the opening of the case oriented opposite to the intended direction of forward travel. The purpose of the orientation was to preserve left/right symmetry for the drivetrain modules.

Figure 3.2: A Pelican case 1400.

Based on the intended footprint, where the Whegs make contact with the ground, external modules were designed to extend the Whegs forward/aft and laterally. This gives MONTe a wide stance which adds to the stability of the platform. There is an o-ring groove, see Figure 3.5, in each attaching module to seal it against the surface where it meets the case. Cutouts in the case allow for wiring and the motors, Figure 3.3.

Figure 3.3: The Pelican case with cutouts for external modules.

Suspension and Drivetrain

The suspension of MONTe consists of radial arms, that project laterally and then forward or aft based on whether they are supporting the front or rear Whegs, called Radial Arms. The Radial Arms contain the drivetrain components and are attached to the drive module, called the Main Drive Assembly, through a hollow 1 inch rotating shaft, Figure 3.4.

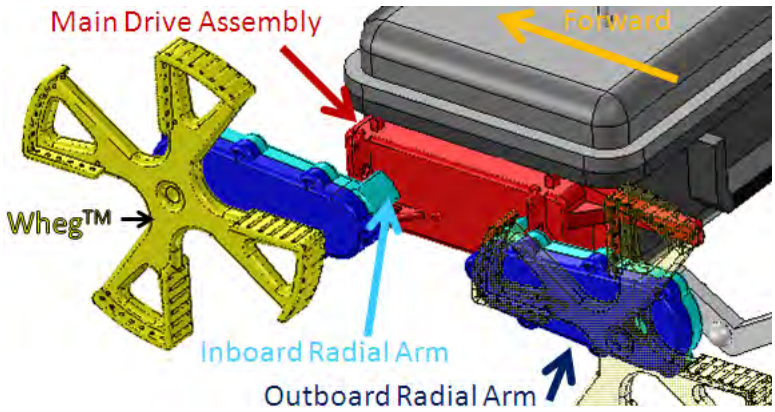

Figure 3.4: A view showing the external assemblies of the suspension.

On the opposite side of the rotating shaft is a lever that is attached to a spring/damper assembly. Motion of the Whegs up and down translates to the extension or compression of the spring/-damper assembly, Figure 3.5. The Radial Arms are able to rotate from zero to 36 degrees. The suspension components were located internally to protect them from harsh environmental conditions as well as prohibit them from snagging vegetation in the water and on land. Bump stops

were added to ensure rotation of the Radial Arms did not exceed 36 degrees, Figure 3.6. 36 degrees equates approximately to three inches of vertical articulation at the Wheg centerline.

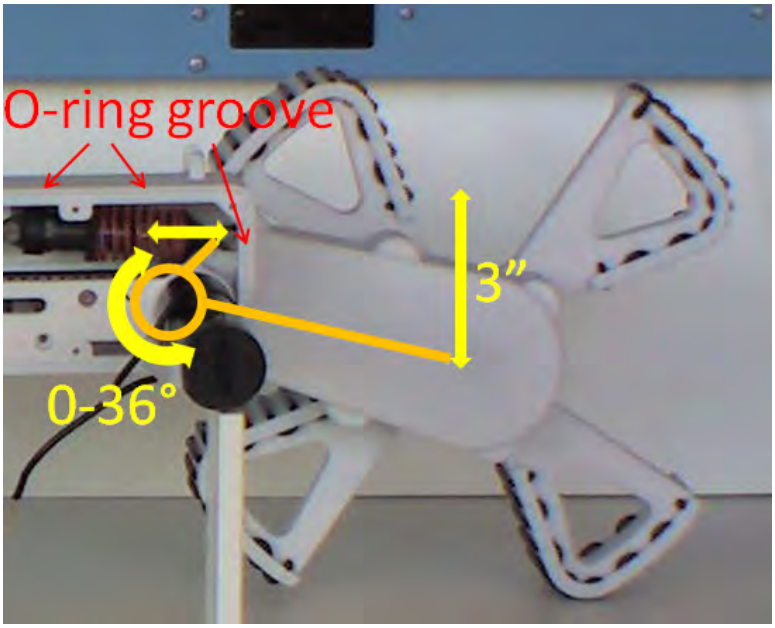

Figure 3.5: A view of the suspension looking within the Main Drive Assembly.

Figure 3.6: Bump stops are mounted where each Radial Arm mounts to the Main Drive Assembly.

The suspension and drivetrain of MONTe are integrated. MONTe maneuvers in a classic tank driven style because the left and right drivetrains are independent. Each drivetrain is actuated by a Maxon 60W DC motor with a permanently mounted 23:1 planetary gear set fixed to the output shaft, Figure 3.7. This gear ratio provides enough torque to move the platform up a 45

degree incline. The motors also have shaft encoders attached to the rear housing, as feedback, for future positioning or dead reckoning schemes.

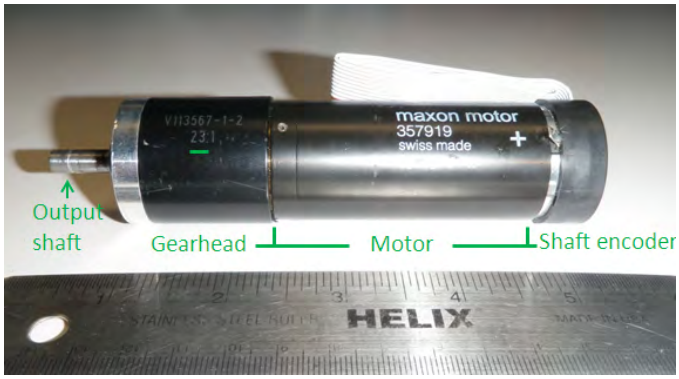

Figure 3.7: Maxon 60W motor with gearhead and shaft encoder.

Torque is transmitted to the front Wheg through a 0.5 inch driveshaft mounted internally to a 1 inch suspension shaft and then through a set of geared pulleys connected by a belt. The end pulley is connected to the Wheg. There is an automatic tensioner that tensions the belt connecting the front and aft drivetrains. There are additional fixed tensioners in the radial arms that serve two functions: ensure proper tension on the belts and route the belt in a fashion that engages additional teeth on the smaller pulley. The final gear ratio is 46:1. The Whegs turn at 178 RPM under no load and nominal motor voltage. Figure 3.8 shows the complete left drivetrain. The right drivetrain is identical.

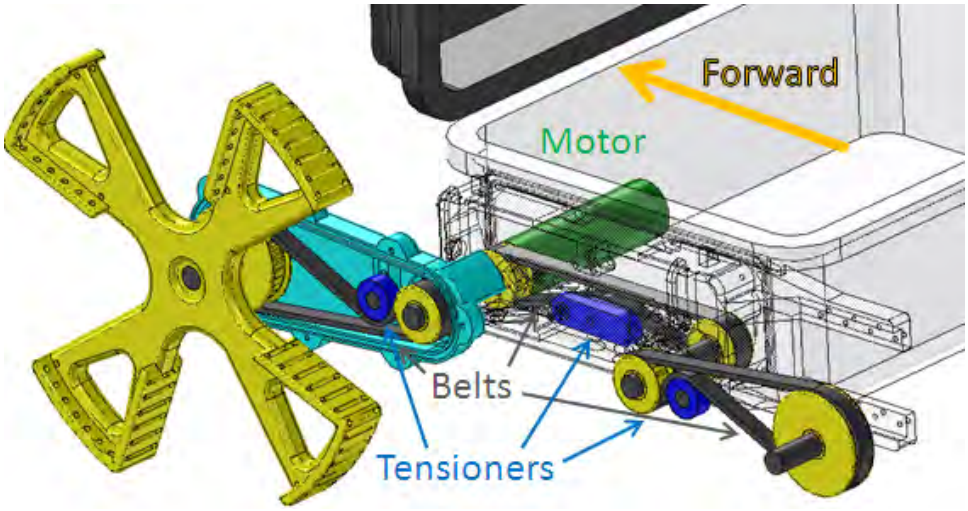

Figure 3.8: Complete left drivetrain.

Tail Integration

The tail design was completed after the design of the suspension and drivetrain. The two main modes of operation included:

- obstacle traverse assistance
- platform self-righting

The traverse assistance mode is the primary reason the tail was added. The tail helps the robot climb obstacles. It also helps the robot turn over when inverted. The results of both modes will be discussed in detail in Chapter 4.

The tail consists of two extensions which each mount in the rear of the Main Drive Assemblies. The left and right side of the tail can move independently from each other, but the current control scheme actuates them as if they were joined. At the end of each tail side, there is a mini-Wheg attached in a manner that limits the rotation to one direction, Figure 3.9. The mini-Whegs help the robot climb without rolling back. The mount location of each tail side allows for approximately 300 degrees of rotation.

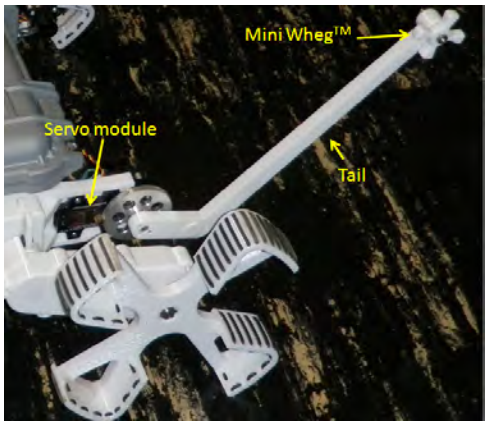

Figure 3.9: Left side of the tail assembly.

If MONTe ends up inverted, the position of the tail determines the corrective action for self-righting. Position 1 shows MONTe upside down with its tail extended, Figure 3.10. The corrective self-righting action for MONTe is to stow the tail while "walking into it". From Position 2, MONTe will unstow the tail, effectively flipping the main chassis back right-side up. A visual depiction of the self-righting modes will be shown in Chapter 4. Servo gearing provides a maximum of 4,300 oz-in of torque. This is enough to flip MONTe over from Position, Figure 3.10.

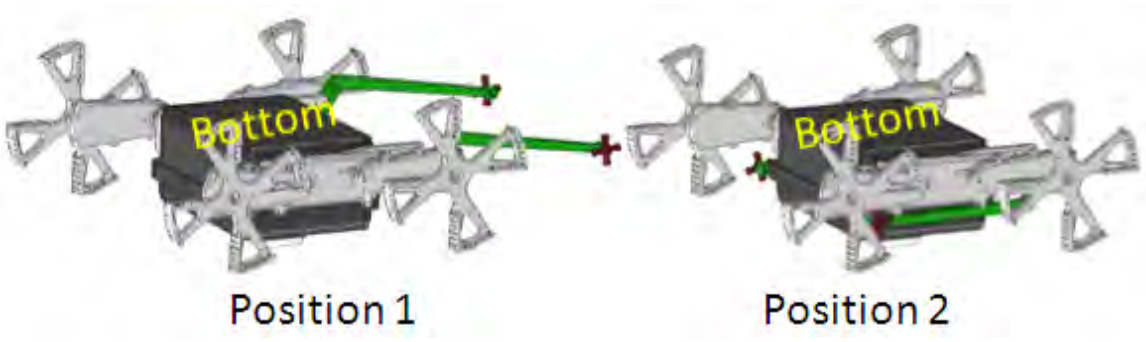

Figure 3.10: Left, Position 1 with tail (green) extended, right, Position 2 with the tail stowed underneath the platform.

Power Control Module

The Power Control Module was designed to locate all the internal mass in the center of the case and to add stability to the platform, Figure 3.11. The module houses the batteries, processors, power supplies and Power Distribution Board. The Power Control Module mounts to an aluminum heat sink that protrudes out the bottom of the case, Figure 3.3. The motor drivers were mounted to the aluminum heat sink for heat dissipation. A better view of the heat sink can be seen in Figure 3.12.

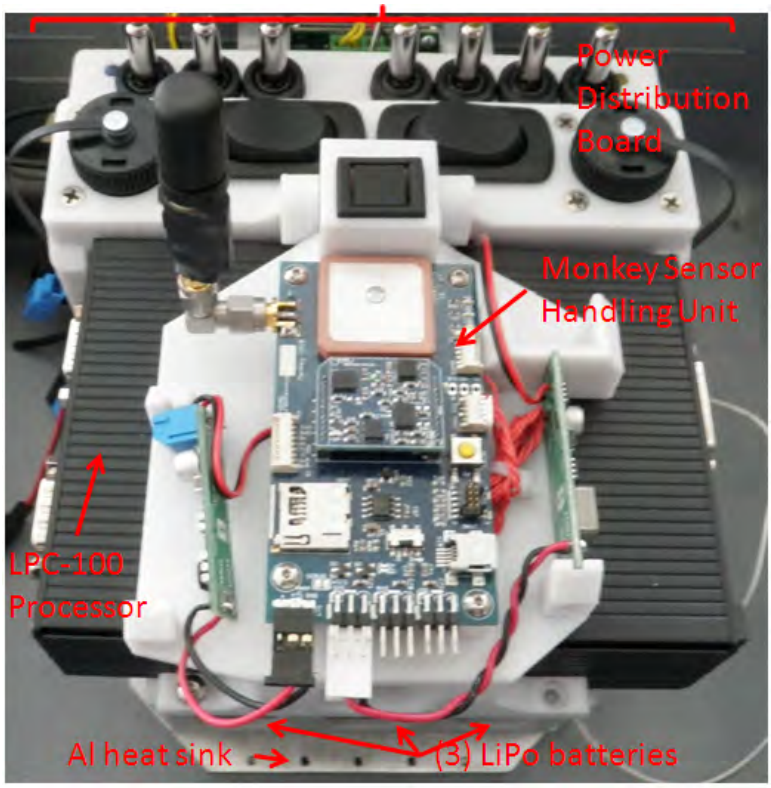

Figure 3.11: The Power Control Module.

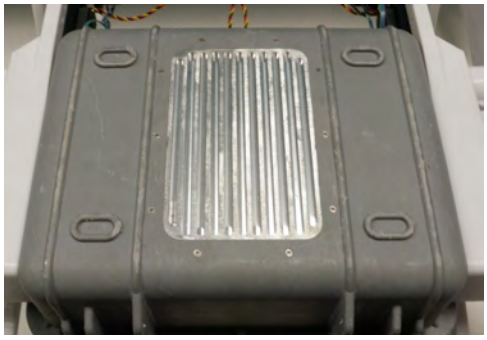

Figure 3.12: The heat sink from an external, bottom up view.

3.2.2 Electronics

Power Distribution

There are two busses that run the electronics onboard MONTe - the power buss and control buss. Both are electrically isolated from each other, which means there are no electrical connections between them. The power buss sources the motor drivers and actuators. The control buss sources the processors, sensors, and other electronic components. Figure 3.13 shows the power distribution scheme used.

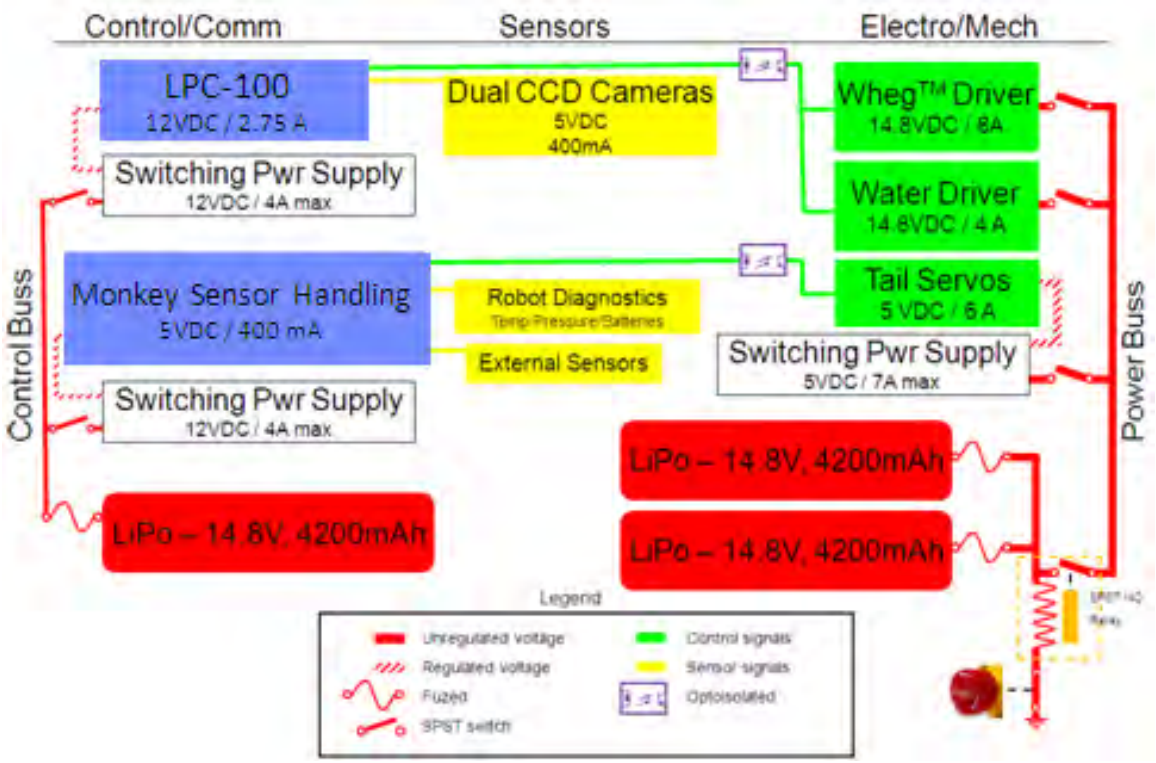

Figure 3.13: Power distribution scheme.

Batteries

The batteries used for MONTe are RC (Lithium-ion Polymer) LiPo batteries from the ThunderPower Prolite series. Each pack is a 4200 mAh 14.8V pack. Each pack is capable of a continuous discharge rate of 63 A. An in line ATO fuse has been added to each pack to prevent inadvertently shorting battery backs, Figure 3.14. There are three identical battery packs onboard MONTe . Two packs are wired in parallel for the power buss and one pack is designated for the control buss, Figure 3.13.

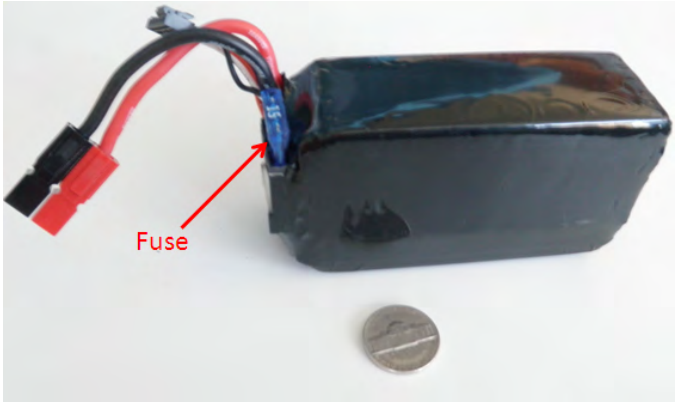

Figure 3.14: One LiPo battery pack.

Switching Power Supplies

Three switching power supplies provide power for the following voltages: regulated 12V/48W for the main LPC-100 processor, regulated 5V/17.5W for the Monkey Sensor Handling Unit and regulated 5V/35W for the tail servos modules, Figure 3.15.

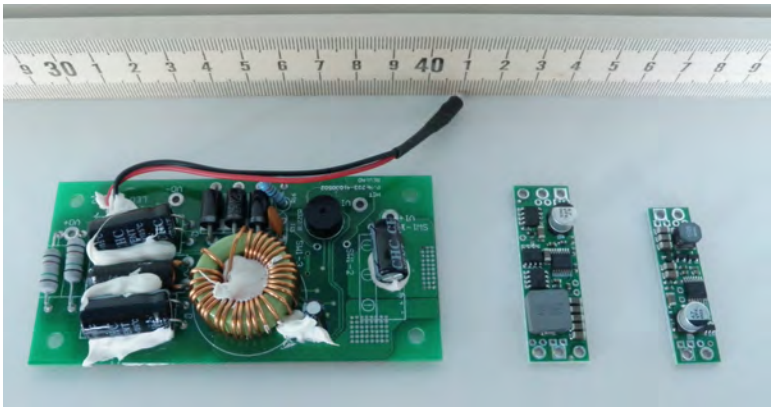

Figure 3.15: From left to right: 12VDC, 5VDC/7A and 5VDC/3.5A.

Motor Drivers

The motor drivers are Dimensional Engineering‘s Sabertooth 2x12. The driver consists of dual 12A PWM drivers capable of peak currents of 25A with an operating voltage range of 6-24V nominal. The particular driver was chosen based on its size, versatility and its long list of options to include the following: four input modes, Lithium protection mode, thermal and over current protection, synchronous regenerative drive, and differential drive mode. The input modes allow for convenient mechanical testing via a standard RC controller as well as a packetized serial mode for higher level schemes. Figure 3.16 is a picture of one driver.

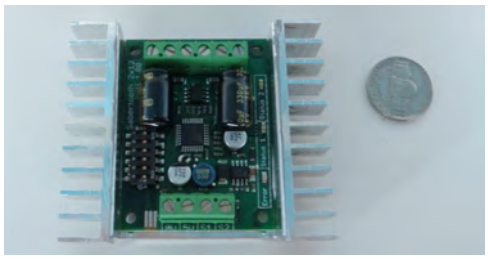

Figure 3.16: Sabertooth 2x12 motor driver.

Main Processor

The main processor is an ultra mini LPC-100 made by Stealth. It consists of a 4.0x6.1x1.45 inch aluminum enclosure that contains a 1.9GHz Dual Core Celeron T3100 processor. The LPC-100 houses multiple ports for communications flexibility, Figure 3.17. The operating system utilized is Ubuntu LINUX.

Sensor Handling Unit

The sensor handling unit is the 2010 Monkey Cortex Navigation Platform with a CHIMU module made by Ryan Mechatronics, Figure 3.17. The backbone of this platform is an ARM Cortex processor that handles the various sensors on board:

- GPS
- barametric pressure
- three axis acceleration
- three axis magnetmeter

The Monkey platform also has ports for RS232/485 and USB communication, external sensor processing and PWM outputs. A micro SD slot is integrated into the module for parameter logging.

Figure 3.17: Left, the LPC-100, right, the Monkey Sensor Handling Unit.

Circuit Board Design

A standard circuit board was designed and etched in an effort to increase the reliability of the power buss. The vibrations experienced in previous platforms showed that protoboard circuits were highly unreliable. The board is a single-sided board etched by the prototype circuit board company PCBSingles.com. The board design incorporates a master switch for each buss and has the following modes: Off, Normal and Battery Charge/External Power. Switches are added to each electrical component to aid in troubleshooting and testing. The power buss also has an emergency mode which secures power to the buss when actuated by an external safety switch, see the lower right corner of Figure 3.13. An additional signal board was created to aid in the noise suppression by optically isolating the control outputs of the LPC-100 and Monkey Sensor Handling Unit from the motor drivers. Figure 3.18 shows a picture of the circuit board while Appendix C includes the trace layout.

Figure 3.18: Power distribution circuit board.

THIS PAGE INTENTIONALLY LEFT BLANK

CHAPTER 4:
Results

MONTe was tested in the field for:

- Vibration performance
- Ruggedness and
- Mobility.

4.1 Vibration Performance

To test the effectiveness of the suspension system, two acceleration data sets were collected on flat terrain. One with the suspension system locked and one with the suspension system enabled. For raw data see Appendix D.

Figure 4.1 shows the suspension in the locked mode.

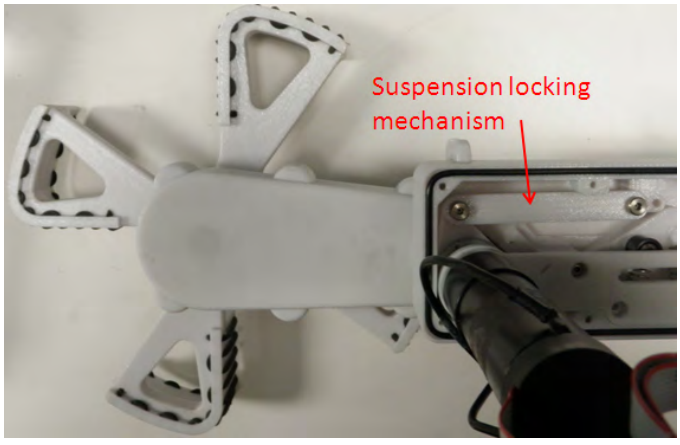

Figure 4.1: Locking mechanism used to prevent the suspension system from moving during testing.

Acceleration data in the z-axis was sampled at 10Hz during each 12 second run. Figure 4.2 shows the raw sampled data.

Notice the smaller standard deviation in the raw data with the suspension enabled which shows that when the suspension is enabled, the main body experiences a decrease in vibrations.

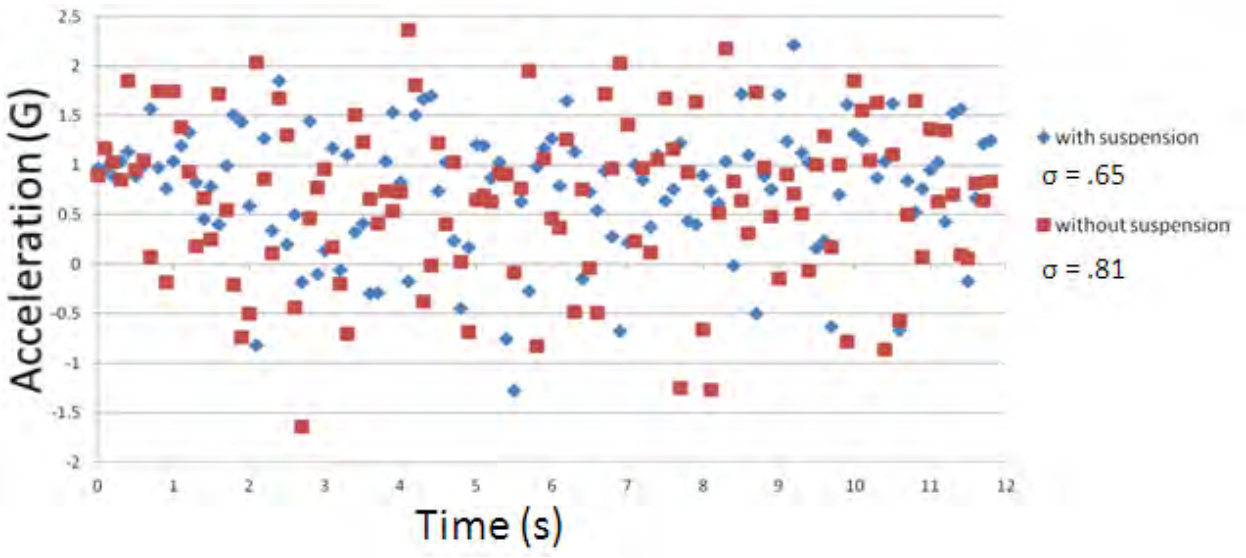

Figure 4.2: Plot of acceleration in vertical axis for an active suspension vs. locked suspension.

Normal Suspension Articulation

An added benefit to the suspension design was the ability to articulate in uneven terrain. Figure 4.3 shows the robot traversing an obstacle. As the left front Wheg drops off the step, the suspension articulates downward to its fully extended position. It contacts the ground sooner than it would if it was fixed in its pre-step position. This increases the net traction used to move the platform.

4.2 Ruggedness

In-field operational tests were conducted to test MONTe's hardware and electronics.

4.2.1 Platform Hardware

Polycarbonate materials used for the fast prototyping of parts via the 3D printing process have proven to be limited for extended use. Multiple part failures were encountered during operational tests. For example, the torque arm that connects the radial arm shaft to the spring/damper assembly has shown a high probability of failure during performance tests at high velocity in rugged terrain. Figure 5.1 shows a picture of the part in discussion and possible future improvements.

4.2.2 Electronics and Inter-Electronics Communications

The primary concern with regard to electronics was excessive heat build-up in the main body compartment during extended operations. Much of this problem was discussed by Halle and

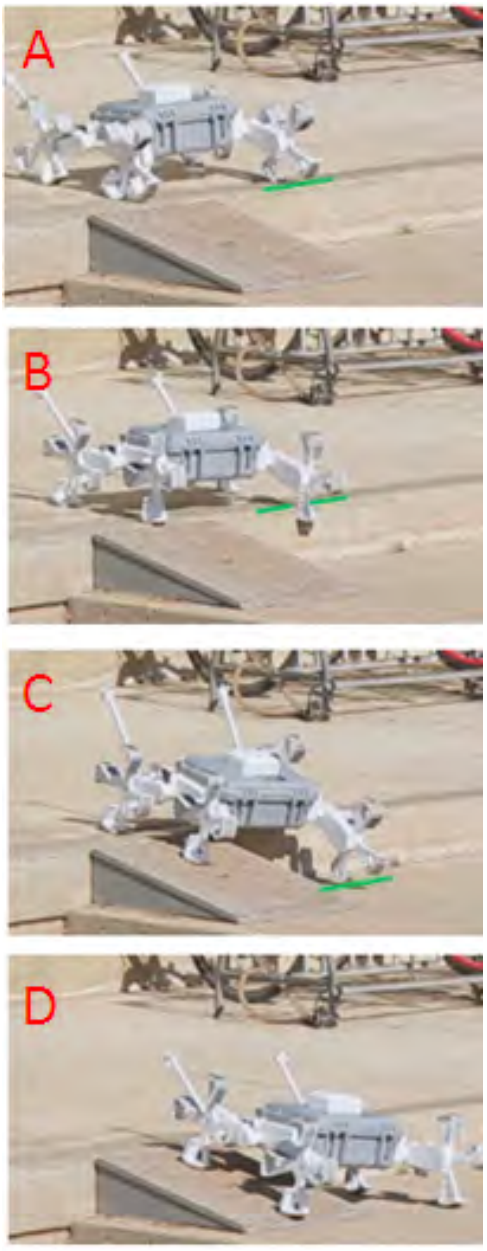

Figure 4.3: Note behavior of front left Wheg as robot traverses the step. The green line shows the step height in A-B and step bottom in C.

Hickle [8]. The solution was to implement a heat sink on the bottom of the platform as discussed in chapter 2.

Early testing revealed that the motors became extremely hot during the first few minutes of operation. They also demonstrated an instability both visual and audible. It was determined that a standing wave on the motor bus needed to be filtered using an inline inductor, [15].

Figure 4.4 shows the difference in temperature caused by the standing wave after 2.5 minutes of normal operation (no external drivetrain load). The unfiltered motor reaches a temperature 7.9 °C above the filtered motor. The filtering scheme keeps the motors cooler preventing damage, which reduces the internal temperature of the platform compared to running them unfiltered.

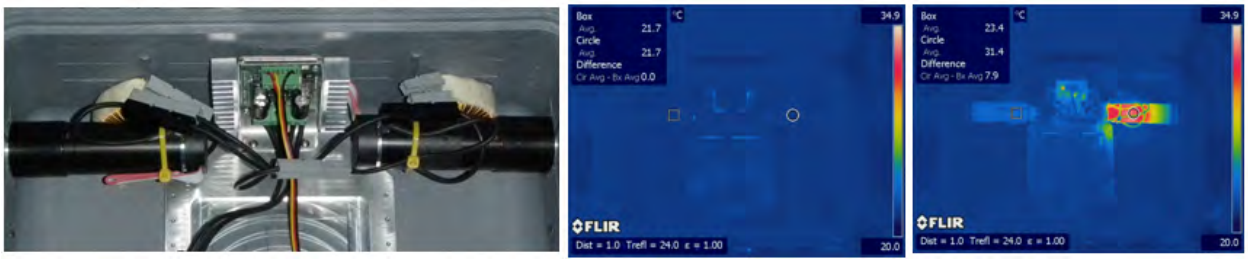

Figure 4.4: Left, visual image shows motor temperature setup (Left motor filtered/Right motor- unfiltered), center, LWIR image shows temperatures at time t=0m, right, image shows temperatures at time t = 2.5m under normal operating speeds with no external load.

In addition to the standing wave produced by the motor driver, the packetized serial mode has also been problematic. The packetized serial mode provides a means to control multiple motor drivers on a shared buss as well as a way to program different functions of the driver such as the ramping mode. The packetized serial mode has worked intermittently and therefore, present autonomous testing uses a slightly less capable serial mode for communications.

In spite of the small problems discussed previously, the electronics and inter-electronic communications on MONTe are functional, modular and have demonstrated ruggedness beyond previous designs.

4.3 Mobility

4.3.1 Drivetrain

The drivetrain of MONTe is functional and modular but design ruggedness remains to be verified. Previous issues associated with drivetrain ruggedness have dealt with the schemes used to transmit torque from the motor to the drivetrain and also from the driveshafts to the pulleys or Whegs. The latest design incorporates a drive pin shown in Figure 4.5. Previously used set screws tended to always vibrate loose and mar the driveshaft they engaged.

4.3.2 Tail Integration

The tail was added to the design mainly for obstacle traversing but also allows the platform to right itself. The size of the tail and control scheme remain in their infancy but the results are discussed below.

Figure 4.5: Drive pin mechanism used to replace previous set screws.

4.3.3 Obstacle Traversing

Figure 4.6 shows MONTe climbing a step with a Wheg diameter:step height of approximately 1:1. The figure is divided into six steps, A-F. Step C shows the platform chassis being held up by the step edge highlighted in green. The tail in Step C is not yet in contact with the ground. Step D shows the rear Whegs being lifted off the ground by the tail that is now in contact with the ground.

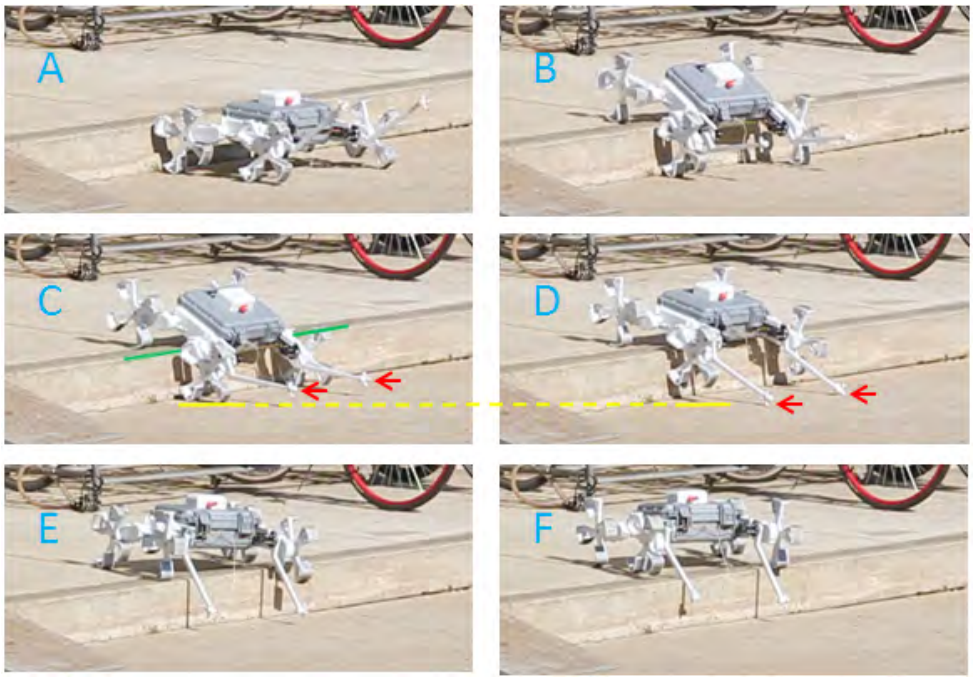

Figure 4.6: MONTe using the tail to traverse an obstacle roughly the same height as the Wheg diameter.

Figure 4.7 shows MONTe attempting to climb a step with a Wheg diameter:step height of approximately 1:1.5. Like Figure 4.6, Figure 4.7 is divided into steps A-F. The rotation of the tail moves MONTe from Step C to Step D, however, is not far enough for the rear Whegs to engage the edge. Although the robot is able to climb higher onto the step with the tail, it is unable to make it over. It is projected that an increase in tail length would help in making it over this particular object. A decrease in separation between the front and rear Whegs would

also help. Based on the results, the use of the tail to traverse obstacles is functional, modular by design and has been surprisingly rugged.

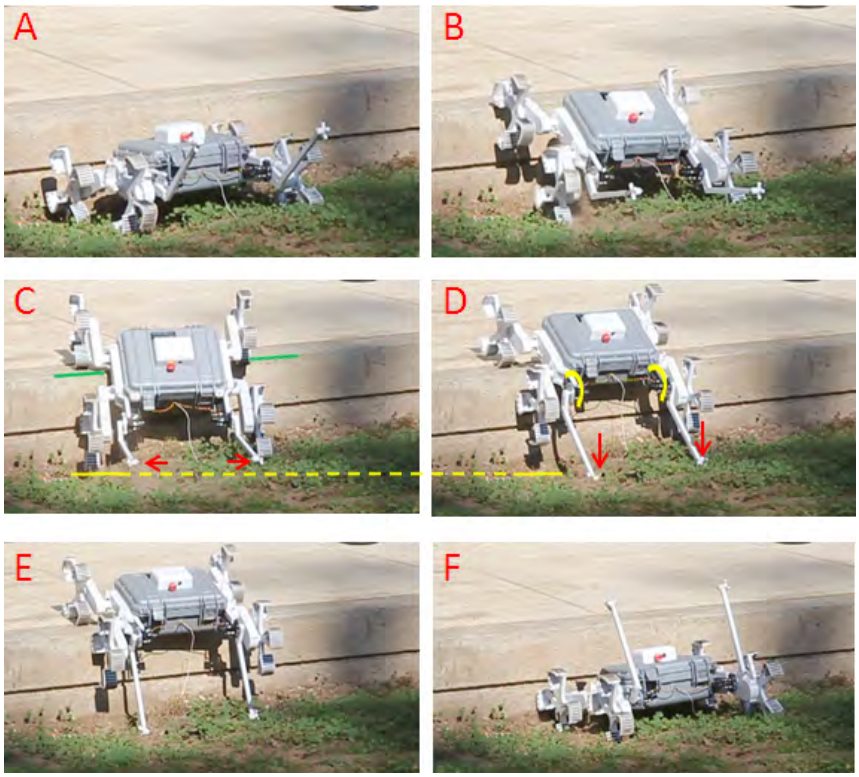

Figure 4.7: MONTe using the tail to traverse an obstacle roughly 1.5 x Wheg diameter.

4.3.4 Self-Righting

The tail is also used in a self-righting mode. Figure 4.8 shows MONTe righting itself from Position 1, which has an intermittent step, Position 2. In the self righting mode, the tail is functional, modular and rugged.

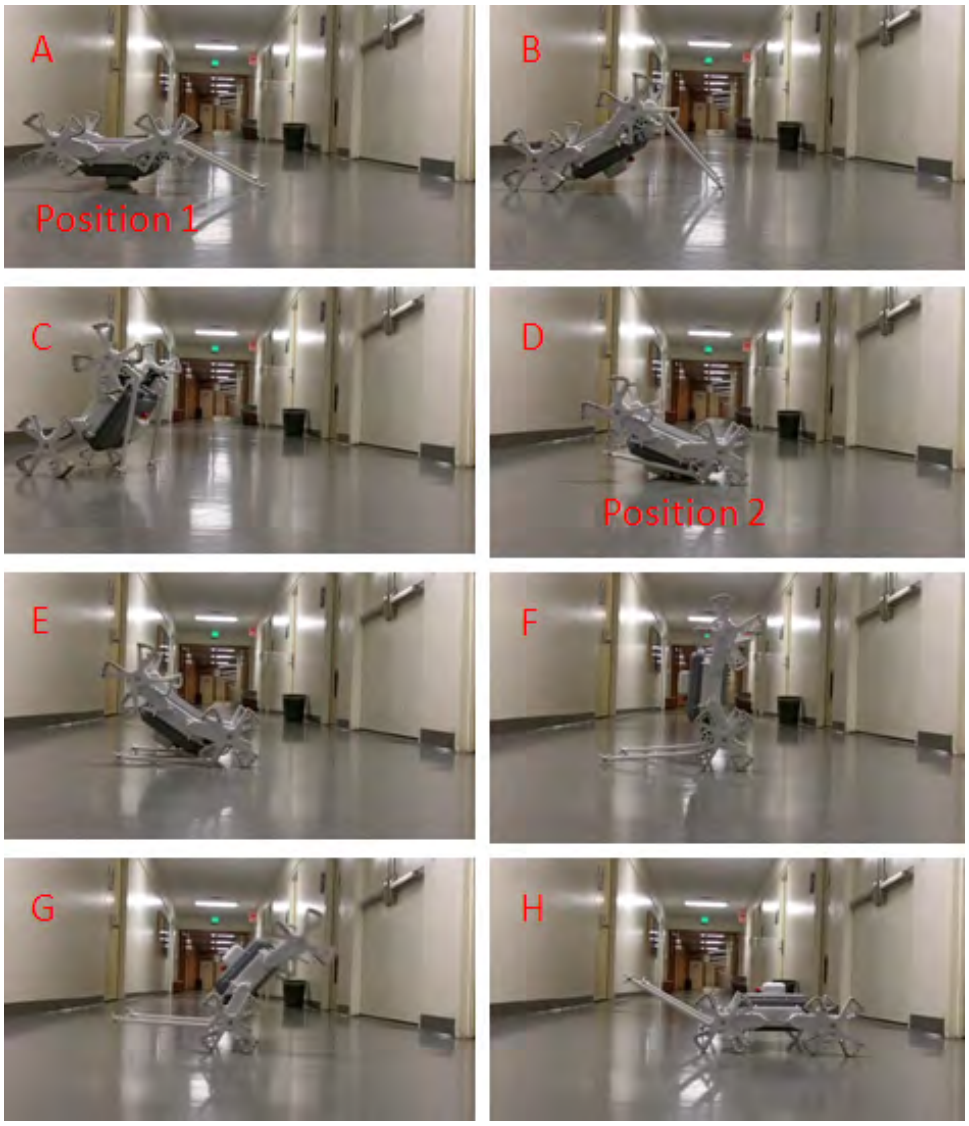

Figure 4.8: A-C shows righting from Position 1, where the tail initially extends beyond the body. D-H show righting from Position 2, where the tail is initially under the body.

THIS PAGE INTENTIONALLY LEFT BLANK

CHAPTER 5:
Future Work

5.1 Torque Arm Upgrade

As discussed in Chapter 4, the torque arm was the weakest link in the mechanical design. It was responsible for approximately 75 percent of the mechanical breakdowns. Future success of the integrated drivetrain and suspension system requires a redesign of that part. Figure 5.1 shows the current two-piece assembly and an IronCAD rendering of one-piece Torque Arm and Radial Arm Shaft machined from aluminum.

Figure 5.1: Left, Torque Arm failed, center, two-piece Torque Arm and Radial Arm Shaft, right, one-piece Torque Transmitting Radial Shaft.

5.2 Waterproofing

Waterproofing MONTe was incomplete due to problems with sealing the modules and drive-shafts. The modularity added to MONTe makes the watertight scheme problematic. There are multiple ways in which water can enter the robot. At each breach point, there is some means to seal the water out, however, the number of breach points is currently 22 (nine for each Main Drive Assembly module, one for the bottom heat sink, one for the top antennae housing, one for the Pelican lid, one for the built in pressure relief valve) and each breach point has an associated reliability coefficient. The waterproofing of the robot needs to work every time and not be a factor of the robot assembler.

There are two types of seals that are not working. The first seal type is the o-ring seal between the Main Drive Assembly Module and the Pelican case, Figure 5.2. The failure in this seal is speculated to be a result of the surface finish of both the external Pelican case and also the

polycarbonate module. The o-ring grove used is not considered a contributing factor to the seal failure based on positive tests completed with the bottom heat sink. The surfaces of the bottom heat sink are the internal Pelican case (considerably smoother than the outside case) and machined aluminum.

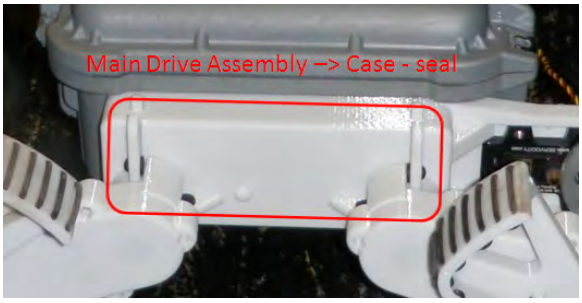

Figure 5.2: The case seal is located between the Main Drive Assembly module and the Pelican case.

The second type of seal which has been problematic is the radial shaft seal used for the rotating Radial Arms and Wheg driveshafts. The polycarbonate surface finish where the seals attach is assumed to be the problem with this type of seal.

Figure 5.3: Radial Arm exposed shaft seal.

Future work to enable MONTe for amphibious operations will include further investigation into proven sealing techniques currently used in industry and robotics. Possible redundant sealing schemes may be of interest which may include waterproofing each electronic device within the case.

5.3 Water-Mobility

The water- mobility scheme for MONTe was never built based on the inability to waterproof the platform. The design called for two “water jets” that would bring water in through the bottom of the platform and accelerate it out of nozzles in the rear of the platform, Figure 5.4. Attaching “water jets” in this manner would create a differential drive similar to the land-borne mobility scheme.

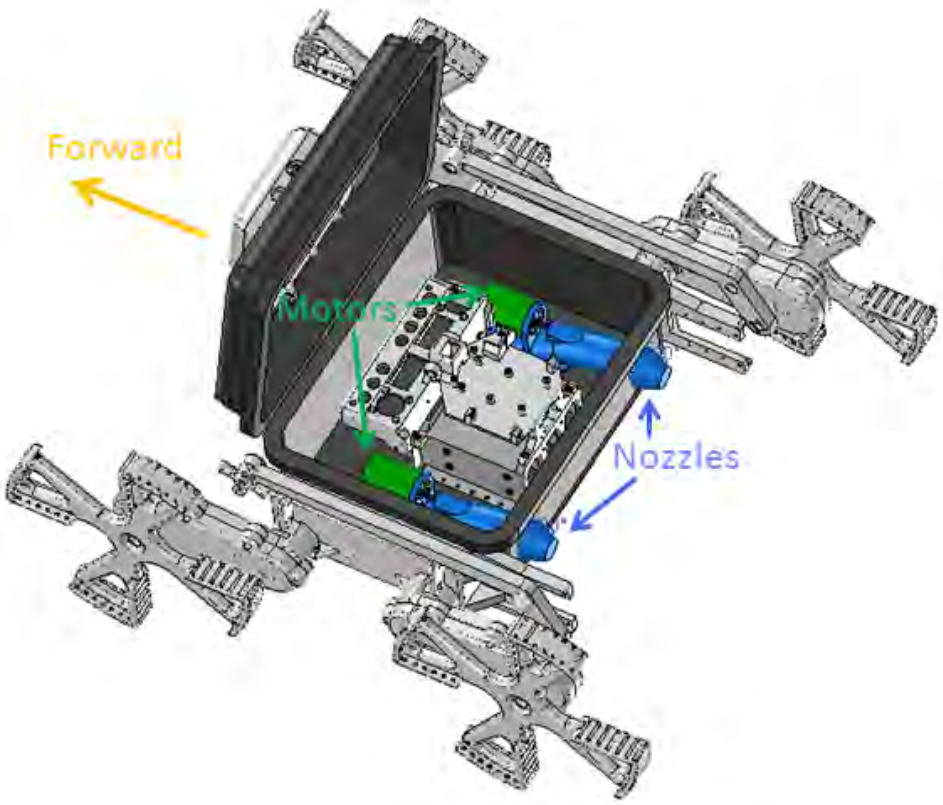

Figure 5.4: IronCAD rendering of “water jets”.

5.4 Onboard Diagnostics

Attempts have been taken to increase the thermal coefficient, G, of the Pelican case by cutting out the bottom of the case and replacing it with an aluminum heat sink panel. Additionally, the efficiency of the power supplies has gone up drastically from previous platforms. Further testing needs to be completed to quantify the results of changes made.

THIS PAGE INTENTIONALLY LEFT BLANK

List of References

[1] T. W. Ferry, "The NPS small robotic technology initiative, man-portable robots for low intensity conflict," M.S. thesis, Naval Postgraduate School, 2001.

[2] J. T. Conway, G. Roughead, and T.W. Allen, "A cooperative strategy for 21st century seapower," Washington, D.C.: U.S. Government, 2007.

[3] J. L. Ward, "Design of a prototype autonomous amphibious whegs robot for surf-zone operations," M.S. thesis, Naval Postgraduate School, 2005.

[4] R. Quinn, J. Offi, D. Kingsley, and R. Ritzmann, "Improved mobility through abstracted biological principles," vol. October, IEEE, 2002, pp. 2652-2657.

[5] T. Dunbar, "Demonstration of waypoint navigation for a semi-autonomous prototype surf-zone robot," M.S. thesis, Naval Postgraduate School, 2006.

[6] A. S. Boxerbaum, M. A. Klein, R. Bachmann, R. D. Quinn, R. Harkins, and R. Vaidyanathan, "Design of a semi-autonomous hybrid mobility surf-zone robot," in *2009 IEEE/ASME International Conference on Advanced Intelligent Mechatronics*, pp. 974-979, Jul. 2009.

[7] C. L. Holland, "Characterization of robotic tail orientation as a function of platform position for surf-zone robots," M.S. thesis, Naval Postgraduate School, 2009.

[8] S. Halle and J. Hickle, "The design and implementation of a semi-autonomous surf-zone robot using advanced sensors and a common robot operation system," M.S. thesis, Naval Postgraduate School, 2011.

[9] J. Rice, B. Creber, C. Fletcher, P. Baxley, K. Rogers, K. McDonald, D. Rees, M. Wolf, S. Merriam, R. Mehio, J. Proakis, K. Scussel, D. Porta, J. Baker, J. Hardiman, and D. Green, "Evolution of a seaweb underwater acoustic networking," in *OCEANS 2000 MTS/IEEE Conference and Exhibition*, 2000, pp. 2007-2017.

[10] McGill University and York University (2008) *Aqua* [Image online], Available: http://www.rutgersprep.org/kendall/7thgrade/cycleA_2008_09/zi/AQUAreading_pic.jpg.

[12] J. R. Taylor, *Classical Mechanics*. Sausalto, California: University Science Books, 2005, vol. Chapter 5.

[13] *Single-Channel: 6N138, 6N139 Dual-Channel: HCPL2730, HCPL2731 – Low Input Current High Gain Split Darlington Optoisolators*, Fairchild Semiconductor Corporation, 2008. [Online]. Available: http://www.fairchildsemi.com/ds/6N/6N138.pdf

[14] K. A. Baravik, "Object localization and ranging using stereo vision for use on autonomous ground vehicles," M.S. thesis, Naval Postgraduate School, 2009.

[15] "PWM low pass filtering application note 32," VOL. 32, 2001. [Online]. Available: http://www.apexmicrotech.ru/pdf/an32u.pdf

APPENDIX A:
MONTe .stl Files (3D Printed Parts)

Appendix A contains a complete list of the 3D printed parts used to create MONTe. Proceeding the file name is the total quantity required to assemble one MONTe.

A.1 Overview

A.2 Main Drive Assembly

A.3 Radial Arm Assembly

A.4 Tail Assembly

A.5 Power Control Module

A.6 Antennae Cover

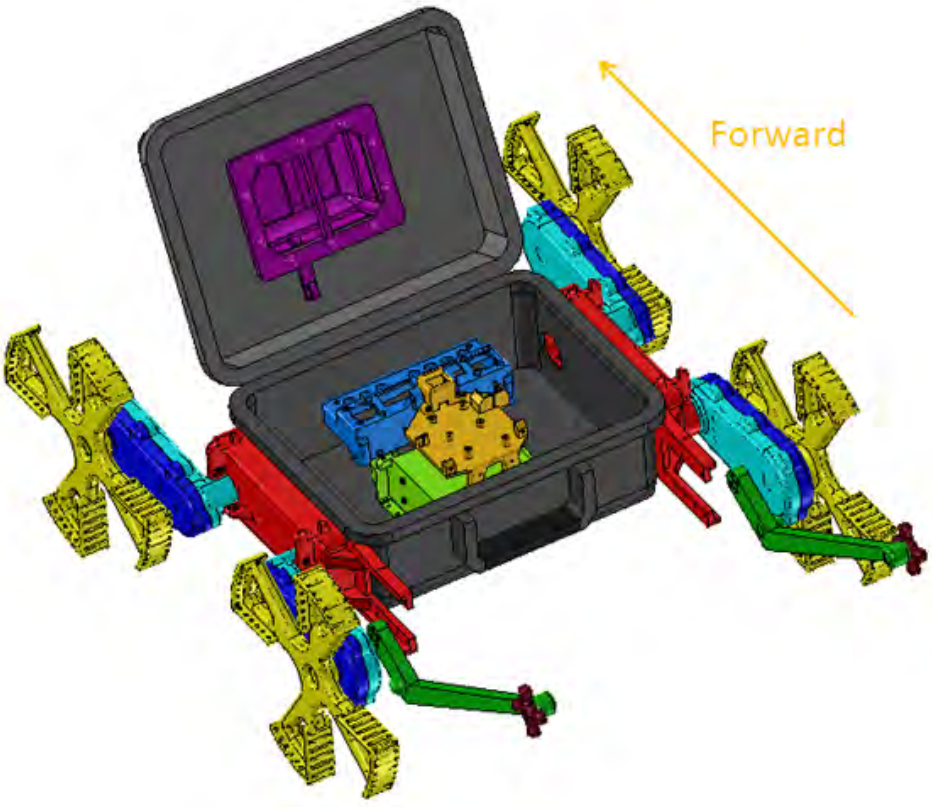

Figure A.1: Overview.

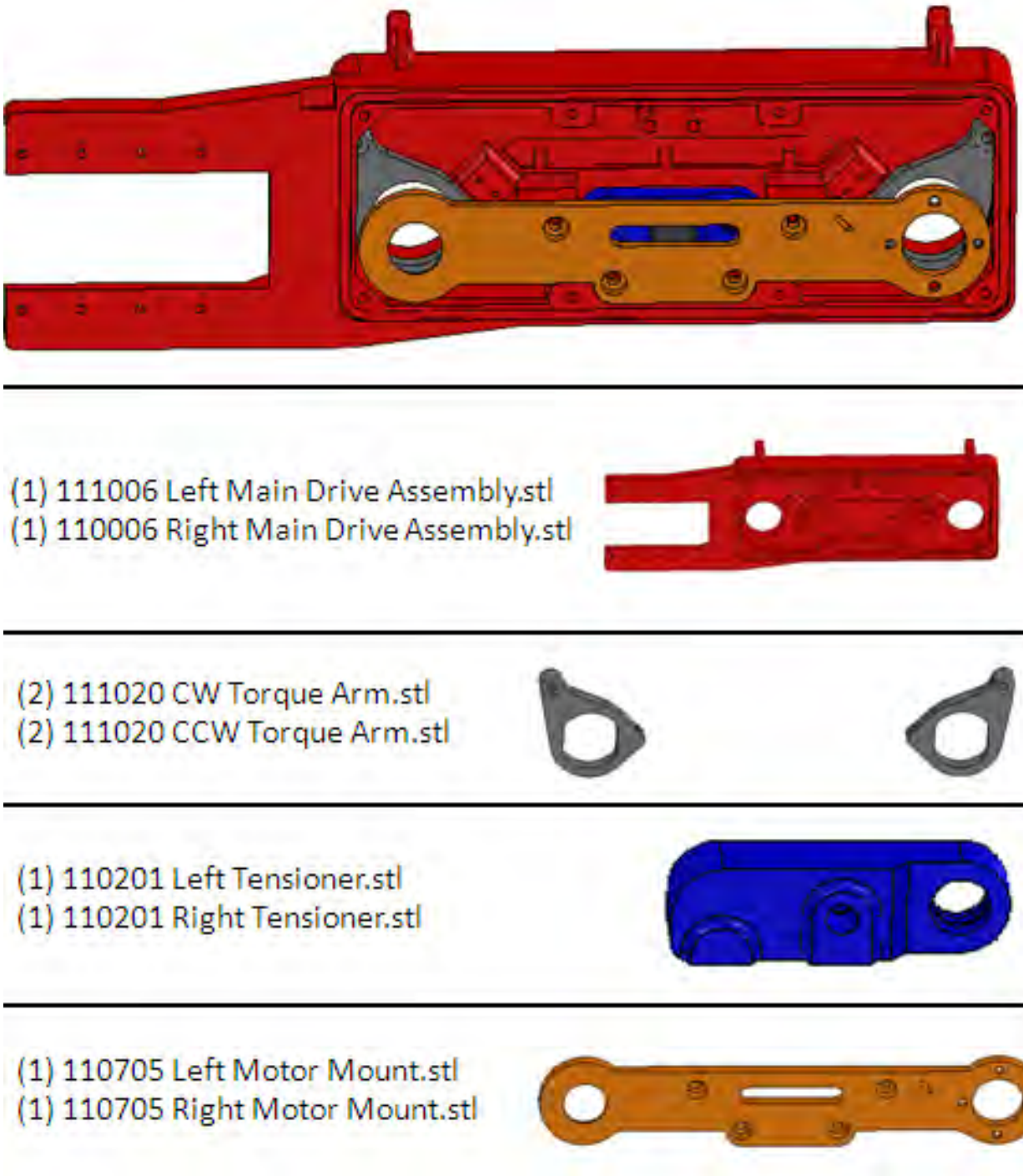

Figure A.2: Main Drive Assembly.

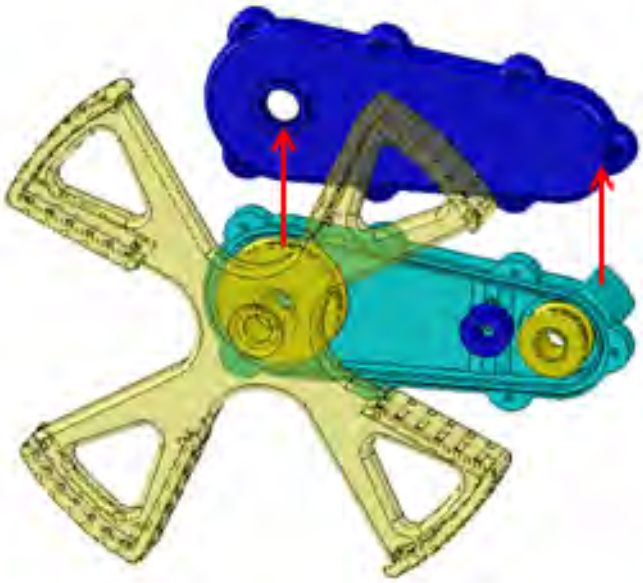

(2) 110814 CW Wheg.stl
(2) 110814 CCW Wheg.stl

(4) 111016 Outboard Radial Arm.stl

(2) 111006 Inboard Radial Arm CW.stl
(2) 111006 Inboard Radial Arm CCW.stl

(4) 111031 32 Tooth Pulley.stl
(4) 111031 16 Tooth Pulley.stl

(4) 111007 Arm Tensioner .9375 Roller.stl

Figure A.3: Radial Arm Assembly.

(1) 111113 Left Tail.stl
(1) 111113 Right Tail.stl

(2) 110814 Tail Wheg.stl

Figure A.4: Tail Assembly.

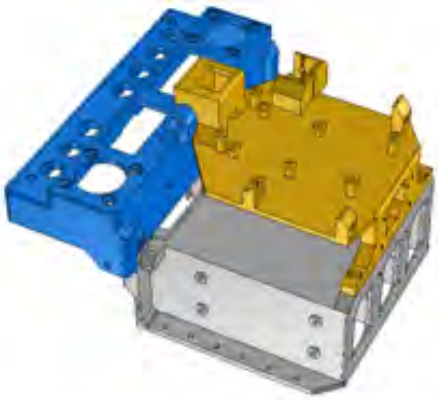

(1) 111113 Power control module Part A.stl

(1) 111113 Power control module Part B.stl

(1) 111118 Power control module Part C.stl

Figure A.5: Power Control Module.

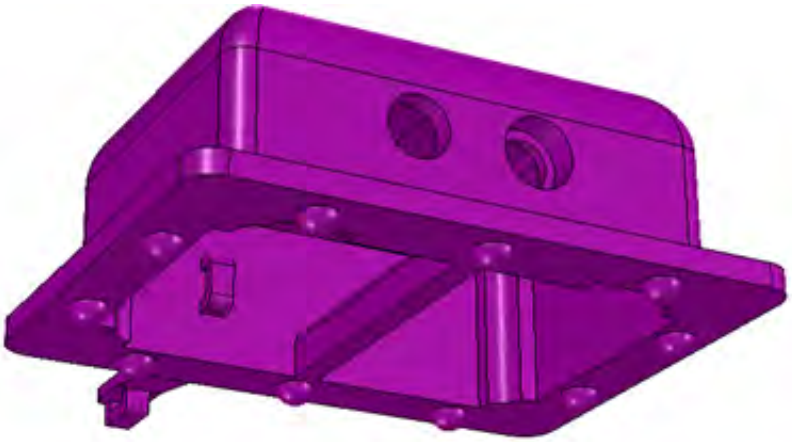

(1) 111007 Antennae cover.stl

Figure A.6: Antennae cover.

THIS PAGE INTENTIONALLY LEFT BLANK

APPENDIX B:
Circuit Board Diagram

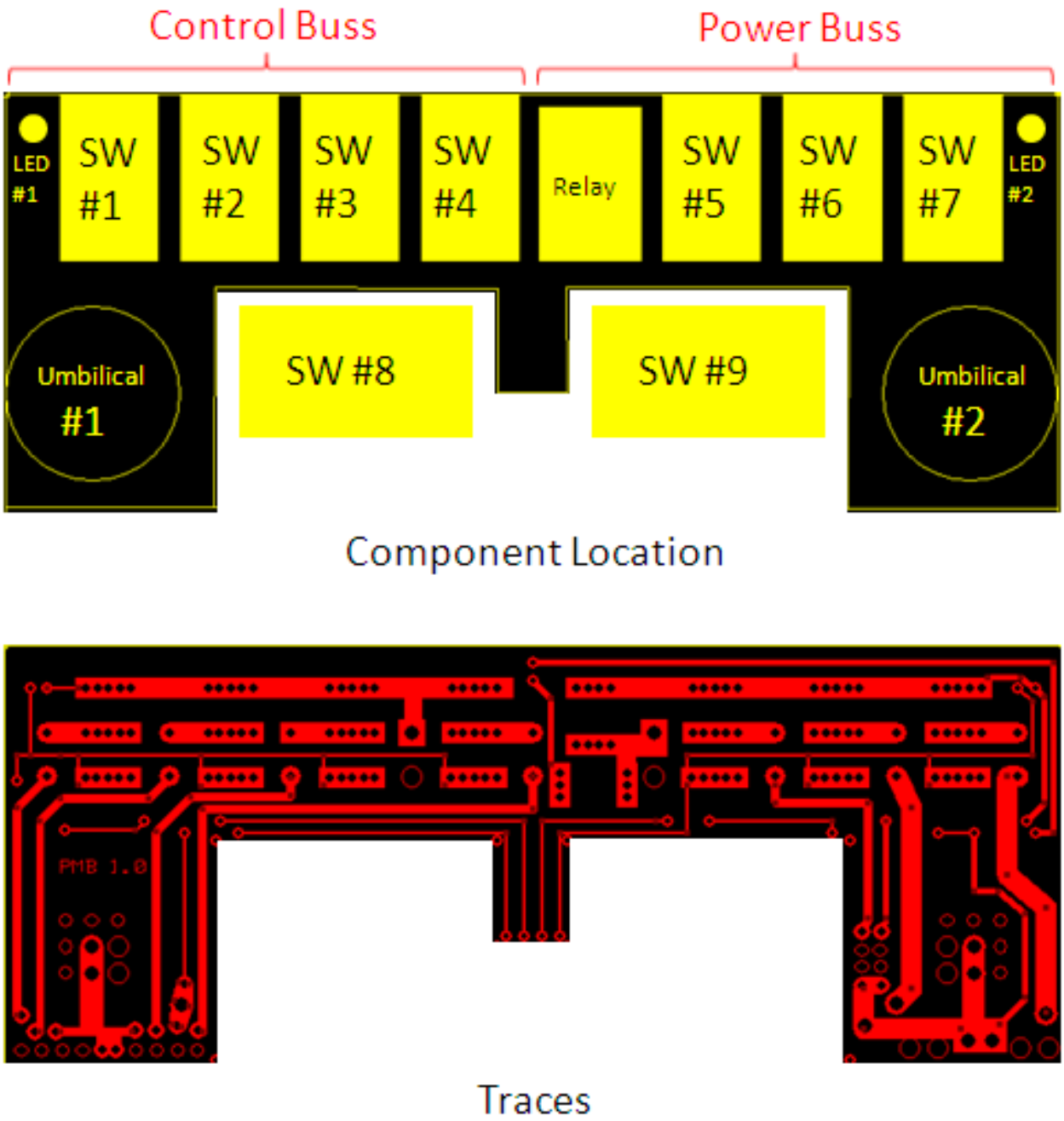

Figure B.1: Circuit board layout.

THIS PAGE INTENTIONALLY LEFT BLANK

APPENDIX C:
Mastercam Heat Sink Files

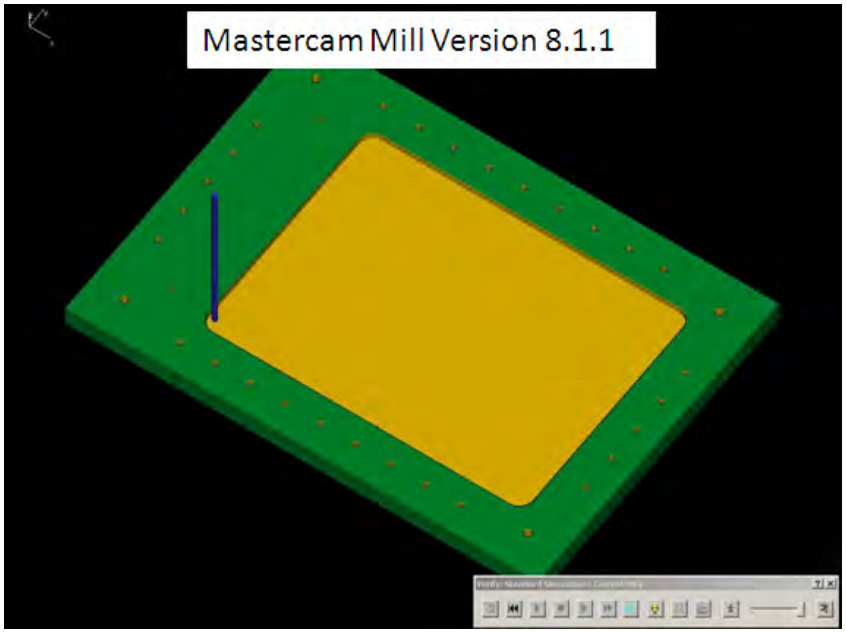

Figure C.1: Mastercam toolpath for the top profile of the heat sink. MONTe Heat Sink Top.mc8

Figure C.2: Mastercam toolpath for the bottom profile of the heat sink. MONTe Heat Sink Bottom.mc8

THIS PAGE INTENTIONALLY LEFT BLANK

APPENDIX D:
Suspension Test Acceleration Data

Time [s]	Vertical accel. with suspension enabled	Vertical accel. with suspension locked
0	-9.490376	-8.851129
0.1	-9.490376	-11.55564
0.2	-8.703609	-10.15421
0.3	-10.1788	-8.433158
0.4	-11.18684	-18.19398
0.5	-8.703609	-9.318271
0.6	-9.81	-10.32632
0.7	-15.41572	-0.737594
0.8	-9.588722	-17.11218
0.9	-7.548045	1.696466
1	-10.20338	-17.18594
1.1	-11.77692	-13.59632
1.2	-13.10459	-9.219925
1.3	-8.162707	-1.794812
1.4	-4.499323	-6.61376
1.5	-7.744737	-2.50782
1.6	-3.958421	-16.91549
1.7	-9.785414	-5.35985
1.8	-14.77647	1.991504
1.9	-14.08805	7.203835
2	-5.77782	4.892707
2.1	7.966015	-20.03797
2.2	-12.44075	-8.482331
2.3	-3.34376	-1.106391
2.4	-18.14481	-16.49752
2.5	-1.966917	-12.78496

Time [s]	Vertical accel. with suspension enabled	Vertical accel. with suspension locked
2.6	-4.94188	4.253459
2.7	1.721053	16.05496
2.8	-14.23556	-4.597669
2.9	0.9834587	-7.646391
3	-1.352256	-9.416616
3.1	-11.55564	-1.770226
3.2	0.5654888	1.942331
3.3	-10.84263	6.884211
3.4	-3.196241	-14.85023
3.5	-4.032181	-12.14571
3.6	2.901203	-6.466241
3.7	2.802857	-4.032181
3.8	-10.22797	-7.253008
3.9	-15.09609	-5.310677
4	-8.162707	-7.154662
4.1	1.622707	-23.20963
4.2	-14.77647	-17.75143
4.3	-16.37459	3.663383
4.4	-16.7188	0.1229323
4.5	-7.228421	-11.9982
4.6	-10.12962	-3.983008
4.7	-2.360301	-10.10504
4.8	4.376391	-0.2458647
4.9	-1.770226	6.638346
5	-11.82609	-6.417068
5.1	-11.8015	-6.810452
5.2	-8.580677	-6.244963
5.3	-10.12962	-8.998647
5.4	7.351354	-8.900301
5.5	12.48993	0.7867669
5.6	-6.269549	-7.548045
5.7	2.581579	-19.12827

Time [s]	Vertical accel. with suspension enabled	Vertical accel. with suspension locked
5.8	-9.711655	8.039775
5.9	-11.55564	-10.44925
6	-12.48993	-4.548496
6.1	-7.769324	-3.663383
6.2	-16.20248	-12.36699
6.3	-11.13767	4.671429
6.4	1.376842	-7.425113
6.5	-7.179248	0.3196241
6.6	-5.409023	4.745188
6.7	-9.293685	-16.8909
6.8	-2.729098	-9.514963
6.9	6.564587	-19.89045
7	-2.163609	-13.81759
7.1	-9.908346	-2.360301
7.2	-8.359399	-9.539549
7.3	-3.712557	-1.204737
7.4	-10.81805	-10.37549
7.5	-6.318722	-16.44835
7.6	-7.425113	-11.40812
7.7	-12.07196	12.24406
7.8	-4.327218	-9.096992
7.9	-4.007594	-16.10414
8	-8.851129	6.392481
8.1	-7.277594	12.39158
8.2	-6.097444	-5.089399
8.3	-10.25256	-21.41481
8.4	0.0737594	-8.261053
8.5	-16.8909	-6.343308
8.6	-10.81805	-3.073308
8.7	4.843534	-17.08759
8.8	-8.777369	-9.613309
8.9	-7.449699	-4.720602

Time [s]	Vertical accel. with suspension enabled	Vertical accel. with suspension locked
9	-16.79256	1.401429
9.1	-12.1703	-8.900301
9.2	-21.73444	-6.982557
9.3	-11.0885	-5.015639
9.4	-10.10504	0.5900752
9.5	-1.622707	-9.859173
9.6	-2.311128	-12.7112
9.7	6.171203	-1.745639
9.8	-6.95797	-9.859173
9.9	-15.8091	7.670978
10	-12.9079	-18.1694
10.1	-12.26865	-15.21902
10.2	-10.1788	-10.27714
10.3	-8.531504	-15.9812
10.4	-10.22797	8.408572
10.5	-15.95662	-10.86722
10.6	6.54	5.507369
10.7	-8.310225	-4.892707
10.8	-5.212331	-16.15331
10.9	-7.498872	-0.8113534
11	-9.367444	-13.42421
11.1	-10.12962	-6.220376
11.2	-4.228872	-13.27669
11.3	-14.97316	-6.908797
11.4	-15.39113	-0.9342858
11.5	1.622707	-0.6392481
11.6	-6.564587	-8.015188
11.7	-11.94902	-6.343308
11.8	-12.26865	-8.261053

Initial Distribution List

1. Defense Technical Information Center
   Ft. Belvoir, Virginia

2. Dudly Knox Library
   Naval Postgraduate School
   Monterey, California

3. Physics Department
   Naval Postgraduate School
   Monterey, California

4. Dick Harkins
   Department of Applied Physics
   Naval Postgraduate School
   Monterey, California

5. Peter Crooker
   Department of Applied Physics
   Naval Postgraduate School
   Monterey, California

6. Ravi Vaidyanathan
   Department of Systems Engineering
   Naval Postgraduate School
   Monterey, California

7. David Price
   GSEAS Military Associate Dean
   Naval Postgraduate School
   Monterey, California